

# Tau Hyperphosphorylation in Synaptosomes and Neuroinflammation Are Associated With Canine Cognitive Impairment

Tomas Smolek,<sup>1</sup> Aladar Madari,<sup>2</sup> Jana Farbakova,<sup>2</sup> Ondrej Kandrac,<sup>2</sup> Santosh Jadhav,<sup>1</sup> Martin Cente,<sup>1,3</sup> Veronika Brezovakova,<sup>1</sup> Michal Novak,<sup>1,3</sup> and Norbert Zilka<sup>1,3,4\*</sup>

<sup>1</sup>Institute of Neuroimmunology, Slovak Academy of Sciences, 845 10 Bratislava, Slovak Republic

<sup>2</sup>University of Veterinary Medicine and Pharmacy, 040 01 Kosice, Slovak Republic

<sup>3</sup>Axon Neuroscience SE, 811 02 Bratislava, Slovak Republic

<sup>4</sup>Institute of Neuroimmunology, n.o., 811 02 Bratislava, Slovak Republic

## ABSTRACT

Canine cognitive impairment syndrome (CDS) represents a group of symptoms related to the aging of the canine brain. These changes ultimately lead to a decline of memory function and learning abilities, alteration of social interaction, impairment of normal house-training, and changes in sleep-wake cycle and general activity. We have clinically examined 215 dogs, 28 of which underwent autopsy. With canine brains, we performed extensive analysis of pathological abnormalities characteristic of human Alzheimer's disease and fronto-temporal lobar degeneration, including  $\beta$ -amyloid senile plaques, tau neurofibrillary tangles, and fused in sarcoma (FUS) and TAR DNA-binding protein 43 (TDP43) inclusions. Most demented dogs displayed senile plaques, mainly in the frontal and temporal cortex. Tau neurofibrillary inclusions were found in only one dog. They were identified with antibodies used to detect tau

neurofibrillary lesions in the human brain. The inclusions were also positive for Gallyas silver staining. As in humans, they were distributed mainly in the entorhinal cortex, hippocampus, and temporal cortex. On the other hand, FUS and TDP43 aggregates were not present in any of the examined brain samples. We also found that CDS was characterized by the presence of reactive and senescent microglial cells in the frontal cortex. Our transcriptomic study revealed a significant dysregulation of genes involved in neuroinflammation. Finally, we analyzed tau phosphoproteome in the synaptosomes. Proteomic studies revealed a significant increase of hyperphosphorylated tau in synaptosomes of demented dogs compared with nondemented dogs. This study suggests that cognitive decline in dogs is related to the tau synaptic impairment and neuroinflammation. *J. Comp. Neurol.* 524:874–895, 2016.

© 2015 Wiley Periodicals, Inc.

**INDEXING TERMS:** canine cognitive impairment; neurofibrillary tangles; tau protein; synapse; microglia; dementia

Canine cognitive impairment syndrome (CDS) represents an unmet medical need in veterinary medicine. It is characterized by deficits in learning, memory, and spatial awareness as well as changes in social interaction and sleeping patterns (Landsberg and Araujo, 2005). A wide variety of age-related changes has been described in the nervous system of senior dogs. Several macroscopic changes such as diffuse thickening of leptomeninges, narrowing of gyri and widening of sulci, ventricular enlargement, and choroid plexus and meningeal fibrosis were observed in old dogs (Borras et al., 1999; González-Soriano et al., 2001). The most prominent microscopic changes were fibrosis of the vessel walls, polyglucosan bodies, astrogliosis (increased GFAP

immunostaining), and meningeal and parenchymal amyloid deposits (Borras et al., 1999).

Senile plaques are located mostly in the cerebral cortex. Amyloid deposition occurs first in the prefrontal cortex and later in entorhinal, temporal, and occipital

T. Smolek and A. Madari contributed equally to this work.

Grant sponsor: Slovak Research and Development Agency; Grant numbers: APVV 0206-11; APVV 0200-11; APVV 0677-12; Grant sponsor: EU Structural Fund; Grant number: 26240220046.

\*CORRESPONDENCE TO: Norbert Zilka, PhD, Institute of Neuroimmunology, Slovak Academy of Sciences, Dubravská 9, 845 10 Bratislava, Slovak Republic. E-mail: norbert.zilka@savba.sk

Received April 7, 2015; Revised July 28, 2015;

Accepted July 30, 2015.

DOI 10.1002/cne.23877

Published online August 27, 2015 in Wiley Online Library (wileyonlinelibrary.com)

© 2015 Wiley Periodicals, Inc.

lobes and occasionally in the cerebellum (Borras et al., 1999; Head et al., 2000; Cotman and Head, 2011). Vascular amyloid angiopathy and  $\beta$ -amyloid deposits are an age-dependent process starting at the age of  $\sim$ 8 years and increasing linearly with age. However, in terms of plaque density, great individual variations were observed in aged animals. Cluster analysis indicated the presence of three subgroups of dogs according to the number of detectable plaques (Czasch et al., 2006). These findings support the role of genetic background in the development of diffuse plaques in dogs (Russell et al., 1996; Wegiel et al., 1996). Finally, senile plaques do not appear to progress beyond the diffuse plaque stage. Most investigators have been unable to detect later-stage thioflavine- or Congo red-positive plaques in canine brains (Giaccone et al., 1990; Uchida et al., 1992a,b; Okuda et al., 1994). On the other hand, classic/neuritic plaques stained either by the silver method or by Congo red have been observed in some previous studies of the canine brain (Russell et al., 1992; Shimada et al., 1991; Rofina et al., 2003).

Several independent studies have demonstrated that the extent of  $\beta$ -amyloid deposition correlates with a decline in select measures of cognitive function (Cummings et al., 1996; Head et al., 1998; Colle et al., 2000; Rofina et al., 2006; Pugliese et al., 2006). Increased  $\beta$ -amyloid accumulation in the frontal cortex and reduced frontal lobe volume correlated with impaired performance on measures of executive function (Tapp et al., 2004). Furthermore, Colle et al. (2000) showed that  $\beta$ -amyloid deposition correlated with changes in maintenance behavior (eating, drinking, autostimulatory behavior, elimination behavior, sleep) but not with environment-dependent symptoms (such as learned specific behavior, self-control, learned social behavior, and adaptive capabilities).

Many studies have failed to detect neurofibrillary tangles in dogs, indicating that tangles are not a regular and consistent feature of the aged canine brain. Usually, Gallyas and Congo red histological methods do not detect any tau deposits, including the neuritic component of plaques, neurofibrillary tangles, or neuritic threads in canine brain. On the other hand, immunohistochemistry has revealed the presence of neurons with tau deposits, indicating the early stage of tangle development (Colle et al., 2000; Pugliese et al., 2006). These results demonstrate that intracellular accumulation of abnormal tau occurs rarely in the brain of aged dogs and is not a prerequisite for cognitive alteration.

The question remains of whether other pathological lesions characteristic of human neurodegenerative disorders such as fused in sarcoma (FUS) and TAR DNA-binding protein 43 (TDP43) inclusions are present in

CDS brain. TDP43 binds both DNA and RNA and is involved in the regulation of transcription, RNA splicing and translation, and neuronal plasticity (Wang et al., 2008). FUS belongs to the TET family of RNA-binding proteins. Even though TDP43 and FUS are localized predominantly in the nucleus, they also can participate in cellular processes in the cytosol (Fontana et al., 2015).

In contrast to  $\beta$ -amyloid and tau pathology, less is known about neuroinflammation and immunosenescence in the aged dog brain. Although Borras et al. (1999) did not find any morphological changes in microglial cells, Hwang and colleagues (2008) showed increased numbers of activated microglia in the dentate gyrus, where the cytoplasm of ionized calcium-binding adapter molecule 1 (Iba1)-immunoreactive microglia was hypertrophied, with bulbous, swelling processes. There was no relationship between microglia and diffuse plaques in aged dog brains. Diffuse plaques usually do not contain glial cells (Uchida et al., 1993; Rofina et al., 2003).

Finally, several studies have reported significant decreases in neuron numbers with age in the cingulate gyrus, superior colliculus, claustrum, and hilus of the hippocampus (Ball et al., 1983; Morys et al., 1994; Siwak-Tapp et al., 2008). Pugliese et al. (2004) showed that calbindin-positive GABAergic interneurons in the prefrontal cortex of the canine brain are also vulnerable to aging. It was hypothesized that synapse loss might also contribute to cognitive decline, but this has not yet been examined in the dog (Siwak-Tapp et al., 2008).

The goal of the present study was to identify novel hallmarks of canine cognitive decline with special emphasis on proteins involved in neurodegeneration in human frontotemporal lobar degeneration such as tau, FUS, and TDP43. To unravel the role of synaptic damage in canine cognitive decline, we analyzed tau phosphoproteome in synaptosomes.

## MATERIALS AND METHODS

### Clinical examination

We examined 215 dogs aged from 8 to 16.5 years, 116 males and 99 females of different breeds and body weights. To rule out medical causes of behavioral decline (Landsberg et al., 2012), all dogs used for this study were assessed by neurological examination, orthopedics, X-ray, ultrasound, and electrocardiogram (ECG) examination as well as blood and urine analyses. An integral part of the diagnosis was neurological and ophthalmic examination as well as hematological (red and white cells and platelets counts; 26 parameters in total) and biochemical (ALT, AST, ALP, pAMS, LIP, Crea, UREA, Glu, Chol, TP, Alb, Ca, P, Mg, NH<sub>3</sub>, K, Na, Cl)

blood tests. Other examinations (such as orthopedics, X-ray, ultrasound, and ECG) were performed when indicated by clinical status or symptoms. Dogs found to have systemic illness that could interfere either with their cognitive status or with testing procedures, such as blindness, deafness, diabetes mellitus, Cushing syndrome, urinary tract infection, incontinence of urine or feces, cardiological problems, head trauma, and other disease conditions, were excluded from the study.

### Behavioral examination

Behavioral investigation included observation of geriatric dogs by a trained investigator and collection of information provided by pet owners. We investigated the neurobehavior of the dog (e.g., apathy, anxiety, staring blankly, confused or aimless walking, excessive vocalization, aggression and anxiety symptoms, signs of compulsive and stereotyped behavior), addressing the various commands, monitoring response to owner and family members, watching behaviors toward outsiders (clinical staff) or other dogs/animals, and monitoring the behavior of the dog during handling. The investigator was proactive in asking about behavioral abnormalities to identify even subtle signs that often go unrecognized by pet owners. Collected data were instrumental for completion of the questionnaire and for the final score calculation. The questionnaire used in this study was adapted from Osella et al. (2007). Based on their cognitive status, the animals were classified into two groups, nondemented controls (with cognitive score up to 15 points, zero to three affected domains, age 1–9 years) and dogs with cognitive deficits (with cognitive score higher than 16 points, four or five affected domains, age 10–19 years).

### Dog samples

The study was performed on the brains of 28 dogs, 17 males and 11 females, of various breeds and from 1 to 19 years of age. In all cases, we obtained fully informed consent from pet owners. Euthanasia was justified for medical reasons; the animals were killed with an intravenous overdose of sodium thiopental (75 mg/kg; Thiobarbital). All animals were treated according to European legislation on animal handling and experiments (86/609/EU). We adhered to a high standard of veterinary care to ensure that all studied dogs received the best care available. All efforts were made to minimize animal suffering.

### Antibody characterization

Anti-tau antibody against phosphoepitope S199 was used (Life Technologies, Grand Island, NY; S199, catalog No. 44734G, RRID:AB\_10835359). The antiserum

raised in rabbit was produced against a chemically synthesized phosphopeptide derived from the region of human tau that contains serine 199. The sequence is conserved in mouse and rat. The antibody recognizes multiple phosphorylated isoforms of tau protein at ~62–75-kDa on Western blots of human, mouse, and rat brain extracts. Recombinant human tau (catalog No. PHB0014) phosphorylated with GSK-3 $\beta$  can be used as a positive control.

Anti-tau antibody against phosphoepitope T205 was used (Life Technologies; catalog No. 44738G, RRID:AB\_10835360). The antiserum raised in rabbit was produced against a chemically synthesized phosphopeptide derived from the region of human tau that contains threonine 205. The sequence is conserved in mouse and rat. This antibody recognizes multiple phosphorylated isoforms of tau protein at ~62–75 kDa on Western blots of human, mouse, and rat brain extracts. Recombinant human tau (catalog No. PHB0014) treated with GSK-3 $\beta$  serves as a positive control for Western blots.

Anti-tau antibody against phosphoepitope T212 raised in rabbit was used (Life Technologies; catalog No. 44740G, RRID:AB\_10836080). The antiserum was produced against a chemically synthesized phosphopeptide derived from the region of human tau that contains threonine 212 (tau 441). The sequence is conserved in mouse, rat, baboon, rhesus monkey, cow, and goat. The antibody recognizes multiple phosphorylated isoforms of tau protein at ~62–75 kDa on Western blots of human, mouse, and rat brain extracts. Recombinant human tau (catalog No. PHB0014) treated with GSK-3 $\beta$  serves as a positive control for Western blots.

Anti-tau antibody against phosphoepitope S214 raised in rabbit was used (Life Technologies; catalog No. 44742G, RRID:AB\_10838932). The antiserum was produced against a chemically synthesized phosphopeptide derived from the region of human tau that contains serine 214 (tau 441). The sequence is conserved in mouse, rat, baboon, rhesus monkey, cow, and goat. The antibody recognizes multiple phosphorylated isoforms of tau protein at ~62–75 kDa on Western blots of human, mouse, and rat brain extracts. Recombinant human tau (catalog No. PHB0014) treated with GSK-3 $\beta$  serves as a positive control for Western blots.

Anti-tau antibody against phosphoepitope 217 was used (Invitrogen, Carlsbad, CA; catalog No. 44-744, RRID:AB\_1502121). The antiserum raised in rabbit was produced against a chemically synthesized phosphopeptide derived from the region of human tau that contains serine 217. The sequence is conserved in mouse, rat, rhesus baboon, monkey, cow, and goat. The antibody recognizes multiple phosphorylated isoforms of tau protein at ~62–75 kDa on Western blots of human,

mouse, and rat brain extracts. Staining of tissue sections from Alzheimer's disease (AD) brain and transgenic rat model (Filipcik et al., 2012) using phospho-tau antibodies S217 antibody detected neurofibrillary tangles and neuritic threads. Insoluble tau extracts from AD brains are used as appropriate positive controls against the antibody.

Anti-tau antibody against phosphoepitope S262 raised in rabbit was used (Life Technologies; catalog No. 44750G, RRID:AB\_10835803). The antiserum was produced against a chemically synthesized phosphopeptide derived from the region of human tau that contains serine 262. The sequence is conserved in mouse, rat, baboon, monkey, cow, and goat. The antibody recognizes multiple phosphorylated isoforms of tau protein at ~62–75 kDa on Western blots of human, mouse, and rat brain extracts. Recombinant human tau (catalog No. PHB0014) treated with PKA or African green monkey kidney (CV-1) cells stably expressing human 4R tau can serve as a positive control for Western blots.

Anti-tau antibody against phosphoepitope S396 raised in rabbit was used (Life Technologies; catalog No. 355300, RRID:AB\_10838933). The antiserum was produced against a chemically synthesized phosphopeptide derived from the region of human tau that contains serine 396. The sequence is conserved in mouse, rat, rhesus baboon, monkey, cow, and goat. The antibody recognizes multiple phosphorylated isoforms of tau protein at ~62–75 kDa on Western blots of human, mouse, and rat brain extracts. Recombinant human tau (catalog No. PHB0014) treated with GSK-3 $\beta$  serves as a positive control.

Anti-tau antibody against phosphoepitope S404 was used (Life Technologies; catalog No. 44758G, RRID:AB\_10851016). The antiserum raised in rabbit was produced against a chemically synthesized phosphopeptide derived from the region of human tau that contains serine 404. The sequence is conserved in mouse, rat, rhesus baboon, monkey, cow, and goat. The antibody recognizes multiple phosphorylated isoforms of tau protein at ~62–75 kDa on Western blots of human, mouse, and rat brain extracts. Recombinant human tau (catalog No. PHB0014) treated with GSK-3 $\beta$  serves as a positive control for Western blots.

A monoclonal antibody against modified tau protein DC11 was previously characterized by Vechterova et al. (2003). The antibody recognizes neither native healthy tau nor its full-length recombinant counterpart. However, the mAb shows strong immunoreactivity with truncated tau (residues t151–421). On immunohistochemistry, the mAb recognizes neurofibrillary tangles, neuropil threads, and neuritic plaques in AD brain tissues. Human AD brain sections serves as a positive control for immunohistochemistry.

The anti-human PHF-tau mAb clone AT8 (Thermo Pierce, Fairlawn, NJ; catalog No. MN1020, RRID:AB\_223647) was raised in mouse against partially purified human PHF-tau. The antibody stained a pattern of neurofibrillary morphology identical to that in previous reports on the aged dog brain (Papaioannou et al., 2001). The antibody detects PHF-tau (Ser202/Thr205) with a predicted molecular weight of ~79 kDa. Human AD brain sections were used as a positive control for histochemical analysis.

Anti-human PHF-tau mAb clone AT180 was raised in mouse against partially purified human PHF-tau (Thermo Pierce; catalog No. MN1040, RRID:AB\_223649). The antibody labels phosphorylated Thr231-stained tau neurofibrillary pathology (Filipcik et al., 2012). HEK293 cells stably express human-tau 4R/2N and serves as a positive control.

A monoclonal antibody against  $\beta$ -amyloid raised in mouse was used (clone 4G8; Covance Research Products, Berkeley, CA; catalog No. SIG-39220-200, RRID:AB\_662810). The antibody was raised against synthetic peptide corresponding to amino acids 17–24 of the human  $\beta$ -amyloid peptide with Glu substituted at position 11, conjugated to KLH. The antibody recognizes abnormally processed isoforms as well as precursor forms of amyloid protein. The antibody stained diffuse amyloid-positive plaques in dog brains, exactly as previously reported (Wegiel et al., 1996). Human AD brain sections were used as a positive control for histochemical analysis.

A mouse monoclonal antibody (IgG1 subtype) to the synaptophysin-1 raised against electrophoretically purified synaptophysin 1 was used (Synaptic Systems GmbH; catalog No. 101011C3, RRID:AB\_887822). The antibody reacts to synaptophysin 1 in human, rat, and mouse among mammals, with a weaker reaction in birds, reptilia, amphibian, and zebrafish. and recognizes a single band of the expected molecular size of ~36 kDa (Jadhav et al., 2015) on Western blots of rat cortical synaptosomes. Purified recombinant synaptophysin acts as a positive control for Western blots.

A polyclonal anti-tau antibody (Poly tau; Axon Neuroscience, Bratislava, Slovakia) raised in rabbit against recombinant human tau protein recognizes all six tau isoforms in both phosphorylated and nonphosphorylated states at ~55–70 kDa in rat synaptic fractions (Jadhav et al., 2015). Recombinant human 6 isoforms serve as a positive control (Jadhav et al., 2015) for Western blots.

A  $\beta$ -tubulin monoclonal antibody (DC126) raised against porcine tubulin in mouse recognizes a single band of ~55 kDa on Western blots of rat cortical synaptosomes or total extract (Jadhav et al., 2015).

Recombinant porcine  $\beta$ -tubulin protein or human tubulin extract or rat brain extracts (Jadhav et al., 2015) acts as a positive control.

A mouse monoclonal antibody (clone 11-9) raised against disease-modified TDP43 protein in mouse (Cosmo Bio, Tokyo, Japan; catalog No. TIP-PTD-M01) was generated against phosphopeptide pS409/410 [SMDSKS(p)S(p)GWG], corresponding to amino acid residues 404–413 of human TDP43 and phosphorylation of serine residues 409/410 (Neumann et al., 2009). The antibody strongly stains TDP43-positive inclusions in brains of patients with frontotemporal lobar degeneration and amyotrophic lateral sclerosis but did not stain normal TDP43 in nuclei (Inukai et al., 2008). TDP43 brain sections were used as a positive control for histochemistry.

Rabbit polyclonal Iba1 antibody was raised against a synthetic peptide corresponding to the C-terminus of Iba1 specific to microglia and macrophage but not cross-reactive with neuron and astrocyte (Wako Chemicals USA; catalog No. 019-19741, RRID:AB\_839504). The antibody raised in rabbit is widely used to study microglial morphology and phagocytosis (Kanazawa et al., 2002) and detects both dystrophic and reactive microglia on immunohistochemistry (Stozicka et al., 2010). Synthetic Iba-1 protein serves as a positive control and detects a  $\sim$ 17 kDa protein on Western blots.

Anti-rabbit drebrin polyclonal antibody raised in rabbit was generated against synthetic peptide conjugated to KLH, corresponding to amino acids 22–42 of human drebrin (Abcam, Cambridge, MA; catalog No. ab11068 RRID:AB\_2230303). The antibody recognized drebrin E isoforms of  $\sim$ 95–120 kDa on Western blot, as previously reported (Xiao et al., 2014; Jadhav et al., 2015). HeLa cell line (ab7898) or rat (E16) spinal cord serves as a positive control.

Anti-rabbit GAP43 antibody raised in rabbit reacts to C-terminal peptide (residues KEDPEADQEHA) of rat and mouse GAP43 protein (Novus Biologicals, Littleton, CO; catalog No. NB300-143, RRID:AB\_10001196). The GAP43 protein is a neuronal marker. The antibody recognizes a prominent band at  $\sim$ 43 kDa, representing the full-length GAP43 protein by Western blot. Cow cerebellum homogenate acts as a positive control.

Monoclonal actin antibody was raised in mouse (Abcam, catalog No. ab76548, RRID:AB\_1523076; clone AC-40) against synthetic peptide within human actin aa 365–375 (C-terminal sequence SGPSIVHRKCF). The antibody recognizes a single band at  $\sim$ 42 kDa on Western blots of dog brains (manufacturer's technical information), as previously reported for rat (Jadhav et al., 2015). Mouse kidney whole-cell lysate serves as a positive control.

Anti-FUS rabbit polyclonal antibody (Sigma Aldrich, St. Louis, MO; catalog No. SAB4200454) was raised

against synthetic peptide corresponding to the N-terminal region of human FUS isoform 1 conjugated to KLH. Anti-FUS antibody labeled neuronal inclusions by immunohistochemistry in a frontotemporal lobar degeneration (FTLD) patient (Neumann et al., 2009). Human brain sample from FTLD was used as a positive control.

### Immunohistochemistry on paraffin sections

The brains were removed according to a standard protocol. Brains were postfixed in 4% PFA for several weeks, embedded in paraffin, and cut on a microtome (Leica RM2255). Immunohistochemical analyses were performed on 8- $\mu$ m paraffin-embedded sections of the prefrontal cortex and hippocampus. Section were treated with formic acid (98%) and heat pretreatment, followed by incubation with primary antibodies against tau, FUS, TDP43, and  $\beta$ -amyloid (4G8; Table 1). All sections were incubated with biotinylated secondary antibody at room temperature for 1 hour and then reacted with avidin-biotin-peroxidase complex for 1 hour. The immunoreaction was visualized with VIP (Vectastain Elite ABC Kit; Vector Laboratories, Burlingame, CA) and counterstained with methyl green (Vector Laboratories). Gallyas silver staining methods were used to demonstrate mature neurofibrillary pathology in neurons as proposed by Gallyas (1971). In all human cases used as a control, informed consent was obtained. Human brain tissue slides were provided by Prof. Irina Alafuzoff (TDP43 case).

### Immunohistochemistry on cryosections

Brains were removed and postfixed in 4% PFA for several weeks. Brain tissues were cryoprotected by infiltration with 15%, 25%, and 30% sucrose. Cryoprotected tissue was embedded with OCT embedding media and immersed into the chilled isopentane cooled by liquid nitrogen. After freezing in the isopentane, tissue was quickly placed on dry ice and finally stored at  $-80^{\circ}\text{C}$  until use. Thereafter, the frozen tissues were sagittally sectioned on a cryostat (Leica) into 50- $\mu$ m coronal sections and collected into six-well plates containing PBS. Sections were incubated with primary antibodies against  $\beta$ -amyloid (4G8) and Iba1 (Table 1), followed by biotinylated secondary antibodies (Vectastain ABC kit; Vector Laboratories). The reaction product was visualized using avidin-biotin and VIP as the chromogen (Vector Laboratories), and sections were mounted on gelatin-coated slides.

### Double-labeling immunofluorescence and confocal microscopy

Paraffin sections were incubated at  $4^{\circ}\text{C}$  overnight with the monoclonal antibody 4G8 and with polyclonal antibody against Iba1 (Table 1). After being washed in

**TABLE 1.**  
Primary Antibodies Used

Antibody	Species raised/ clonality	Description of Immunogen	Source, catalog No., RRID	Dilution
Anti-tau (poly-tau)	Rabbit/polyclonal	Raised against recombinant human six tau isoforms	Axon Neuroscience (Bratislava, Slovakia)	1:1 <sup>1</sup>
Anti- $\beta$ -tubulin (DC126)	Mouse/monoclonal	Porcine tubulin	Axon Neuroscience (Bratislava, Slovakia)	1:1 <sup>1</sup>
Antisynaptophysin-1	Mouse/monoclonal	Electrophoretically purified synaptophysin	Synaptic Systems GmbH; 101 011C3, RRID:AB_887822	1:3,000
Antidrebrin	Rabbit/polyclonal	Synthetic peptide conjugated to KLH, corresponding to amino acids 22–42 of human drebrin	Abcam; ab11068 RRID:AB_2230303	1:2,000
Anti-GAP43	Rabbit/polyclonal	C-terminal peptide of rat and mouse GAP43, which is KEDPEADQEHA	Novus Biologicals; NB300-143, RRID:AB_10001196	1:2,500
Anti-tau [pS199]	Rabbit/polyclonal	Chemically synthesized phosphopeptide derived from the region of human tau that contains serine 199	Life Technologies 44734G, RRID:AB_10835359	1:1,000
Anti-tau [pT205]	Rabbit/polyclonal	Synthetic phosphopeptide derived from the region of human tau that contains threonine 205	Life Technologies; 44738G, RRID:AB_10835360	1:1,000
Anti-tau [pT212]	Rabbit/polyclonal	Synthetic phosphopeptide derived from the region of human tau that contains threonine 212	Life Technologies; 44740G, RRID:AB_10836080	1:1,000
Anti-tau [pS214]	Rabbit/polyclonal	Chemically synthesized phosphopeptide derived from the region of human tau that contains serine 214	Life Technologies; 44742G, RRID:AB_10838932	1:1,000
Anti-tau [pThr217]	Rabbit/polyclonal	Synthetic phosphopeptide derived from the region of human tau that contains threonine 217	Invitrogen; 44-744, RRID:AB_1502121	1:1,000
Anti-tau [pS262]	Rabbit/polyclonal	Chemically synthesized phosphopeptide derived from the region of human tau that contains serine 262	Life Technologies; 44750G, RRID:AB_10835803	1:1,000
Anti-TAU [pS396]	Rabbit/polyclonal	Purified human PHF-tau preparation	Life Technologies; 355300, RRID:AB_10838933	1:1,000
Anti-tau [pS404]	Rabbit/polyclonal	Chemically synthesized phosphopeptide derived from a region of human tau that contains serine 404	Life Technologies; 44758G, RRID:AB_10851016	1:1,000
Anti-ruman PHF-tau (clone AT8)	Mouse/monoclonal	Phospho-PHF-tau pSer202 + Thr205	Thermo Pierce; MN1020, RRID:AB_223647	1:1,000
Anti-human PHF-tau (clone AT180)	Mouse/monoclonal	Partially purified human PHF-tau	Thermo Pierce; MN1040, RRID:AB_223649	1:1,000
Anti-Iba1	Rabbit/polyclonal	Synthetic peptide corresponding to C-terminus of Iba1	Wako Chemicals USA; 019-19741, RRID:AB_839504	1:500
Anti- $\beta$ -amyloid (clone 4G8)	Mouse/monoclonal	This antibody is reactive to amino acid residues 17–24 of $\beta$ -amyloid; the epitope lies within amino acids 18–22 of $\beta$ -amyloid (VFFAE)	Covance Research Products; SIG-39220-200, RRID:AB_662810	1:1,000
Anti-FUS	Rabbit/polyclonal	Synthetic peptide corresponding to the N-terminal region of human FUS isoform 1 conjugated to KLH	Sigma Aldrich; SAB4200454	1:1,000
Anti TDP43, phospho Ser409/410 (clone 11-9)	Mouse/monoclonal	CMDSKS(p)S(p)GWGM, S(p):phosphoserine 409/410	Cosmo Bio (Tokyo, Japan); TIP-PTD-M01	1:1,000
Antiactin	Mouse/monoclonal	Chicken gizzard actin	Abcam; ab76548, RRID:AB_1523076	1:2,500
Anti-tau (DC11)	Mouse/monoclonal	AD brain extracts, conformational epitope between aa 321 and 391	Axon Neuroscience (Bratislava, Slovakia)	1:1 <sup>1</sup>

<sup>1</sup>Supernatants from cultured hybridoma cells were used.

PBS, the sections were incubated in the dark with secondary antibodies conjugated with Alexa488 or Alexa546 (Molecular Probes, Eugene, OR) at a dilution

of 1:1,000. Finally, sections were mounted in Vectashield mounting medium (Vector Laboratories) and examined with a Zeiss LSM 700 confocal microscope.

## Synaptosome preparation

Synaptosomal fractionation was performed using a well-established protocol for humans (Tai et al., 2012; Chang et al., 2013) rats (Jadhav et al., 2015), dogs (Cohen et al., 1977), and mice (Mondragón-Rodríguez et al., 2012). Briefly, tissues were homogenized in homogenizing buffer containing 0.32 M sucrose, 4 mM HEPES, pH 7.4, with complete protease inhibitors (Roche, Mannheim, Germany) using an Omni TH homogenizer (Omni International, Kennesaw, GA) or a glass homogenizer. After centrifugation of homogenate at 900g, the supernatant obtained was further centrifuged at 9,000g. The resulting pellet was suspended in homogenizing buffer and layered over a discontinuous sucrose gradient (0.8 M, 1.0 M, and 1.2 M) and centrifuged in an MLS 50 rotor (Beckmann ultracentrifuge). The synaptosomes at interface 1.0 M and 1.2 M sucrose were carefully collected. All steps were performed at 4°C, and samples were stored at -80°C until use.

## Sarkosyl fractionation

Sarkosyl insoluble tau was extracted as previously described (Jadhav et al., 2015). Tissues were homogenized in an Omni homogenizer in buffer containing 20 mM Tris, pH 7.4, 800 mM NaCl, 1 mM EGTA, 1 mM EDTA, 10% sucrose, and protease inhibitors. After centrifugation at 20,000g for 20 minutes, the supernatant (S1) was collected. Sarkosyl (40% w/v in water) was added to the final concentration of 1% and stirred for 1 hour at room temperature. The sample was then centrifuged at 100,000g for 1 hour at 25°C in a Beckmann TLA 100. The resulting pellet was washed and used for Western blot analysis.

## Western blotting

Proteins were resolved by 12% SDS-PAGE and transferred to a nitrocellulose membrane. The membranes were blocked in 5% nonfat free milk or BSA in 1 × TBS-Tween. The blots were incubated with primary antibodies (Table 1) in either 5% BSA or 5% fat free milk for 2 hours or overnight at 4°C. After being washed, membranes were incubated with secondary antibodies (Dako, Glostrup, Denmark). Blots were developed with SuperSignal West Pico chemiluminescent Substrate (Thermo Scientific, Schaumburg, IL) on an Image Reader LAS-3000 (Fuji Photo Film Co, Ltd., Tokyo, Japan). The intensity of blots was quantified in Advanced Image Data Analyzer software (AIDA Biopackage Raytest).

## RNA extraction

TRI reagent, a monophasic solution of phenol and guanidine isothiocyanate (Sigma; catalog No. T9424-200ML) was used to isolate total RNA. Tissues from the

frontal cortex (100 mg) of normally aged and CDS-suffering animals were used for transcriptomic analysis. Tissue samples were homogenized in 1 ml TRI reagent in a 1-ml Dounce glass tissue grinder with tight pestle. Briefly, the homogenized samples were incubated for 5 minutes at 25°C to permit the complete dissociation of nucleoprotein complexes, and 0.2 ml chloroform per 1 ml TRI reagent was added. Tubes were vigorously shaken for 15 seconds and incubated at 25°C for 2–3 minutes. The samples were then centrifuged at 12,000g for 15 minutes at 4°C. After centrifugation, the upper aqueous phase containing RNA was retrieved, and 0.5 ml isopropyl alcohol per 1 ml TRI reagent used for the initial homogenization was added to precipitate the RNA in solution. Samples were incubated at 25°C for 10 minutes and centrifuged at 12,000g for 10 minutes at 4°C. The RNA pellet was washed once with 1 ml of 75% ethanol. Samples were mixed and centrifuged at 7,500g for 5 minutes at 4°C. The wash solution was aspirated, and the RNA pellet was briefly dried and redissolved in 100 µl RNase-free water at 58°C for 10 minutes.

## RNA integrity analysis

RNA integrity was analyzed with an Agilent 2100 Bioanalyzer, a microfluidics-based platform, in which the concentration and integrity of extracted total RNA were examined. An RNA 6000 Nano kit (Agilent Technologies, Palo Alto, CA; catalog No. 5067-1511) was used according to the manufacturer's recommendations. Analysis revealed high integrity of RNA, with an RNA integrity number (RIN) of 7.1–8.0, confirming the high quality of all samples used for transcriptomic study.

## Reverse transcription

Synthesis of the first strand was carried out using the RT<sup>2</sup> First Strand kit (Qiagen, Valencia, CA; catalog No. 330401) according to the manufacturer's protocol. Initially, the genomic DNA elimination step was performed according to instructions and 4 µg of each RNA sample was subsequently reversely transcribed into cDNA with a three-step protocol: 42°C for 15 minutes, 95°C for 5 minutes, 4°C indefinitely. After synthesis, 20 µl cDNA samples were stored at -70°C until use.

## Quantitative real-time PCR

Quantitative PCR targeting inflammatory genes of interest was performed using the Dog innate and adaptive immune responses RT<sup>2</sup> profiler PCR array (Qiagen; catalog No. PAFD-052ZA). Composition of the quantitative PCR mix (2,500 µl) for one PCR array plate was as follows: 1,250 µl 2 × RT<sup>2</sup> SYBR Green Mastermix (Qiagen; catalog No. 330523); 1,200 µl nuclease-free H<sub>2</sub>O,

and 50  $\mu$ l cDNA sample (200 ng/ $\mu$ l); 25  $\mu$ l of this mixture was pipetted into 96-well plates containing lyophilized primers for individual genes of interest, housekeeping genes, reverse transcription controls, and PCR amplification controls. Plates were sealed with optical covers and cycled under the following conditions: 95 °C for 10 minutes, followed by 40 cycles of 95 °C for 15 seconds, and 60 °C for 1 minute with an ABI 7500 real-time PCR system (Applied Biosystems, Foster City, CA). Data analysis was performed in ABI 7500 software v.2.0.2 (Applied Biosystems). Comparative  $\Delta\Delta$ Ct analysis was performed to compare fold change of gene expression in CDS-suffering animals over the normal aging control group. RPLP1 gene was used as a housekeeping control.

### Data analysis

All experiments were performed in triplicate to check for consistency of our results. Only one randomly selected value per experiment, however, was used for statistical analysis. Representative blots are shown in figures. Statistical analyses were performed in Matlab (Mathworks, Natick, MA). All values were normalized to values of their loading controls (actin, tubulin), and levels of phosphorylated tau were normalized further to total tau levels. We evaluated the differences between means by using nonparametric bootstrapping (Efron and Tibshirani, 1993; 1,000 bootstrap data replications) on the significance level  $\alpha = 0.05$  and corrected for multiple comparisons (Benjamini and Hochberg, 1995). Analogously, we computed 95% confidence intervals for the differences between means. Use of individual two-tailed *t*-tests to compare differences between phosphorylation levels and protein levels, further corrected for multiple comparisons, provided the same results. Similarly, evaluating regional differences by one-way balanced ANOVA and correcting for multiple comparisons provided the same statistical results. Graphs showing means were generated in Prism (GraphPad Software, San Diego, CA). Error bars show SEM.

## RESULTS

### Diffuse and compact plaques are frequently present in demented dogs

The amyloid precursor protein (APP) sequence of *Canis familiaris* has 98% homology with human APP and an identical amino acid sequence (Johnstone et al., 1991). Therefore, we used monoclonal antibody 4G8, which is reactive to amino acid residues 17–24 of human  $\beta$ -amyloid and cross-reacts with APP. Our immunohistochemical study showed that the frontal and temporal cortex were the most commonly affected sites.

Similarly to previous reports (Colle et al., 2000; Czasch et al., 2006), three types of amyloid deposits were recognized in the demented dogs: condensed, diffuse cloud-like, and perivascular plaques (Fig. 1A). Few animals exhibited both the condensed and the diffuse amyloid deposits, whereas only the diffuse cloud-like plaques were present in all investigated demented canine brains and in some nondemented control cases. From the group of demented subjects we identified dogs with a low (+), medium (++), and high (+++) number of plaques (Fig. 1B–D, Table 2). We did not detect any plaques in the white matter. We also have not observed neuritic plaques with a condensed core of amyloid surrounded by a corona of dystrophic tau-positive neurites characteristic of AD. For nondemented controls, we observed neither condensed plaques nor vascular amyloid deposition. Colocalization study revealed that the majority of plaques did not contain activated or resting microglia (Fig. 1E). Microglial cells inside the amyloid plaques were rare and usually appeared to be in resting form (Fig. 1F).

### Tau, FUS, and TDP43 lesions do not represent hallmarks of canine dementia

Some studies have shown very few tau-positive intraneuronal structures in the brain of aged dogs, suggesting that the presence of neurofibrillary lesions may represent another hallmark of canine dementia (Colle et al., 2000; Pugliese et al., 2006). We analyzed sarkosyl-insoluble tau in all demented dogs used in this study. Soluble tau displayed an identical pattern in all examined brain samples (Fig. 2A). Dog brains expressed four tau isoforms (Janke et al., 1999), so the pattern differed slightly from that of human tau proteome, in which six tau isoforms were identified. No sarkosyl-insoluble tau was detected in the samples analyzed (Fig. 2B).

For rapid immunohistochemical screening, we used mAb AT8 that is sensitive and specific for abnormal tau phosphorylation and is widely used for detection of neurofibrillary lesions in AD (Alafuzoff et al., 2008). We found that only one dog displayed AT8-positive intraneuronal inclusions (dog 16). In this particular case, we performed immunohistochemical analysis of tau pathology with a variety of monoclonal and polyclonal antibodies recognizing different tau phospho-sites. Tau intraneuronal fibrillary structures were distributed in prefrontal and temporal cortex, entorhinal cortex (Pre- $\alpha$  layer and Pri- $\alpha$  layer), and the CA1 sector of hippocampus (Fig. 3A–C). In contrast to previous reports (Colle et al., 2000; Pugliese et al., 2006), our study showed tau-positive fibrillar structures inside principal neurons.

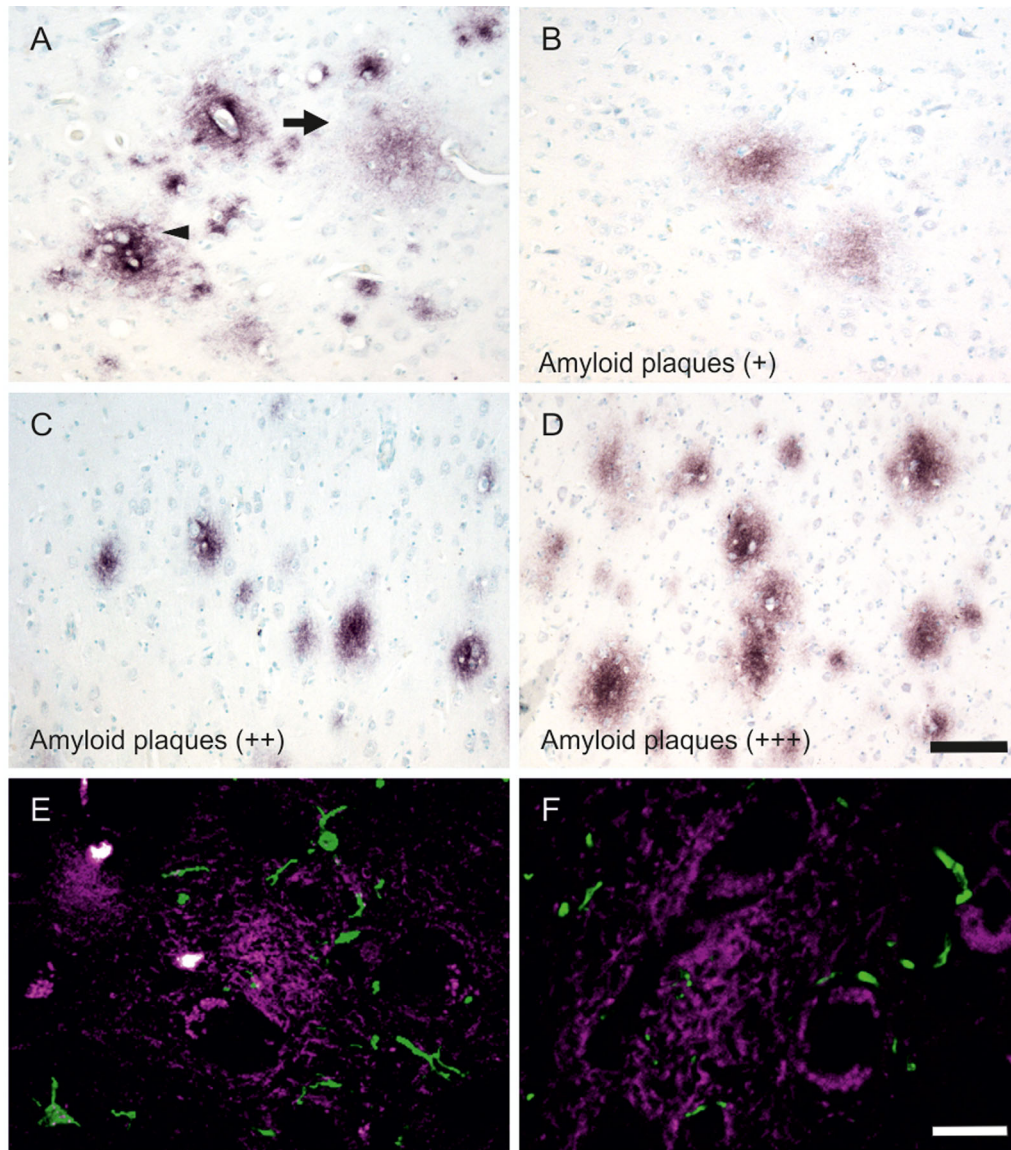


**Figure 1.**  $\beta$ -Amyloid deposition in demented canine brain. Using cryosection immunohistochemistry, we observed two main types of amyloid plaques in the demented canine brain, condensed and diffuse cloud-like. The other type of amyloid lesion is located in the close proximity of capillaries (A). We performed semiquantitative analyses of the number of plaques. For CDS dogs we observed very few plaques of mostly diffuse forms (no more than three per slide; B), moderate numbers of plaques (up to  $\sim$ 30 plaques per slides; C), and extensive numbers of plaques (D). Colocalization study showed that the majority of plaques did not contain microglia (E). Only occasionally did we observe resting microglia randomly distributed within plaques (F). Scale bars = 100  $\mu$ m in D (applies to A–D); 100  $\mu$ m in F (applies to E,F).

Tau pathology was identified with antibodies that are specific for tau protein species hyperphosphorylated at Ser202, Thr205, Thr212, Ser214, Thr217 (not shown), Thr231, Ser235, Ser262 (not shown), Ser396 (not shown), and Ser404 (not shown). Some tangle-bearing neurons were also immunolabeled with antibody DC11, which has been used to detect disease-modified tau in the human brain (Vechterova et al., 2003). We distinguished two types of tau lesions, early, containing rod-like inclusions evenly distributed in somatodendritic compartment (Fig. 3A–D), and late, represented by

fibrils located almost exclusively in the neuronal soma (Fig. 3E–I). The former type did not contain argyrophilic material, whereas the latter type was positive for Gallyas silver staining (Fig. 3H,I) and was immunoreactive for DC11 (Fig. 3G).

In parallel, we analyzed the presence of FUS and TDP43 pathology in serial sections from prefrontal and temporal cortex and hippocampus. We found that anti-FUS antibody recognized physiological intranuclear staining in several neurons (Fig. 4A). Typical small dots were seen in FUS-positive nuclei, representing a normal

**TABLE 2.**  
**Characteristics of Dogs Used in This Study**

No.	Age (years)	Breed	Weight (kg)	Sex	Modified DISHA score (Osella et al., 2007)		Senile plaques hippocampus/ frontal cortex	Microglia
					Points	No. of affected domains		
1	5	Poodle, medium	10	M	0	0	-/-	Resting microglia
2	3	German shepherd	35	M	0	0	-/-	Resting microglia
3	9	American cocker spaniel	11	F	0	0	-/-	Resting microglia
4	1	German shepherd	28	M	0	0	-/-	Resting microglia
5	7	Sharpei	27	M	0	0	-/-	Resting microglia
6	5	Irish wolfhound	64	M	0	0	-/-	Resting microglia, few clusters
8	13	English cocker apaniel	12	M	10	1	-/-	Resting microglia, few clusters
7	10	Rhodesian ridgeback	32	M	15	3	-/-	Resting microglia, few clusters
9	12	Mixed breed	15	M	17	4	-/-	Resting microglia, few clusters
10	9	Poodle, miniature	3	F	18	4	-/-	Activated microglia, cluster
11	10	Poodle	5	F	21	4	-/-	Activated microglia, clusters
12	10	Welsh terrier	9	F	22	4	+/+	Resting microglia, clusters
13	13	Golden retriever	29	M	23	4	+++ / +++	Resting microglia, clusters
14	12	Labrador retriever	26	F	26	4	+++ / +++	Activated microglia, clusters
15	9.5	Rottweiler	52	M	27	5	+/+	Resting microglia
16	13	Pekingese	8	F	27	5	+/+	Dystrophic microglia, activated microglia
17	9	Mixed breed	24.5	F	30	5	+/+	Resting microglia
18	12	Poodle	4.7	F	32	5	+++ / +++	Resting microglia, few dystrophic microglia
19	13	German shepherd	55	M	33	4	+/+	Dystrophic, hypertrophic microglia
20	14	German shepherd	28	M	34	5	+/+	Resting microglia, few dystrophic microglia
21	13	Poodle	8.2	M	37	5	+++ / +++	Resting microglia, few dystrophic microglia
18	13	Golden retriever	35	M	44	5	+++ / +++	Dystrophic and activated microglia
22	12.5	German shepherd	22	F	42	5	+++ / +++	Dystrophic microglia
23	13	Mixedbreed	15	F	46	4	+/+	Dystrophic and hyperramified microglia
24	16	Poodle	5.6	M	47	5	+/+	Dystrophic microglia, clusters
25	16	Poodle	6	M	53	5	+++ / +++	Activated microglia
26	16	German spitz	8	F	60	5	-/+	Dystrophic microglia
27	19	Mixed breed	6.3	M	67	5	+++ / +++	Dystrophic microglia, clusters
28	17	German spitz	10	M	70	5	+/+	Activated microglia

physiological staining pattern (Fig. 4B, inset). FUS-positive nuclei were present in both gray and white matter. No intranuclear or cytoplasmic FUS aggregates were found in any brain sample analyzed. A human sample with intranuclear FUS aggregates was used as a control (Fig. 4C). Antibody used for detection of TDP43-positive aggregates in human patients with FTLD did not recognize any pathological structures in selected brain areas (Fig. 4D,E). Another human sample with cytoplasmic TDP43 aggregates was used as a positive control (Fig. 4F).

### Activated and dystrophic microglia appear frequently in the brain of demented dogs

We proceeded to look at age- and cognitive state-related changes in microglia. Using antibody Iba1, we

found that in nondemented dogs resting microglia are distributed in all tested brain areas. In contrast, with demented dogs, we observed very often activated or dystrophic forms of microglia (Fig. 5A,B). Streit and Braak suggested using thick sections to distinguish between activated and dystrophic microglia, because thin, paraffin-embedded tissue could be insufficient for making a precise morphological study of microglial cells (Streit et al., 2009). Therefore, we used 50- $\mu$ m-thick frozen sections that allowed us to monitor the morphological metamorphosis of microglial cells in aged dog brains. Frequently we observed activated microglia with characteristic enlarged cell processes (Fig. 5C). In many demented dogs, microglial cells displayed features of dystrophy, with spheroidal or bulbous swellings and deramified and/or tortuous processes (Fig. 5D).

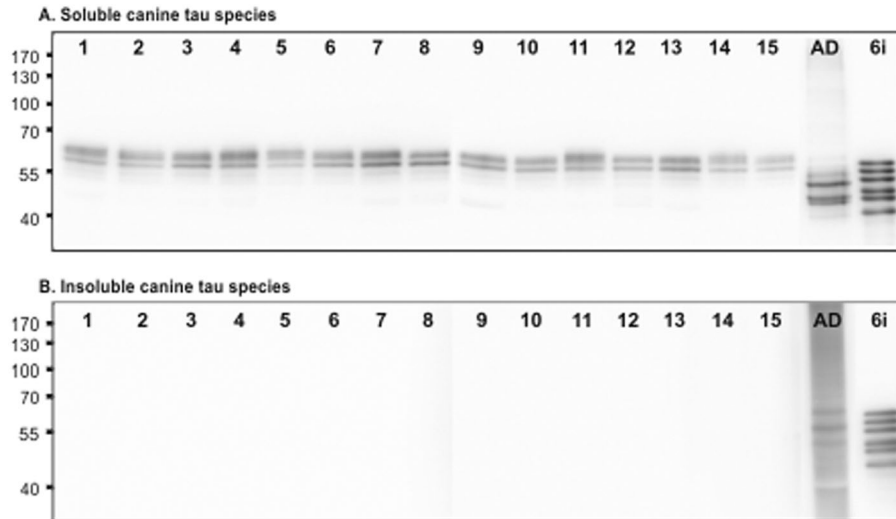


**Figure 2.** Insoluble tau is absent in demented canine brain. We tested 15 demented dogs for the presence of soluble and insoluble tau in the hippocampus and temporal cortex. All examined brain samples showed identical pattern of soluble tau containing four tau isoforms (A). No sarkosyl-insoluble tau was detected in any of demented dogs (B).

The most striking feature of a canine brain affected by dementia is the presence of multicellular aggregates lacking constitutive contact inhibition. As in humans, we recognized early microglia clusters containing ramified, activated microglial cells (Fig. 5E) and late microglia clusters consisting of reactive microglia with short, deramified processes (Fig. 5F). As in human aging, large microglial clusters can measure 250–300  $\mu\text{m}$  at the longest axis.

### Dysregulation of inflammatory genes in CDS brain

To identify the inflammation markers during neurodegeneration, we performed quantitative real-time PCR profiling of 84 genes associated with innate and adaptive immunity. Quantitative comparison of gene expression profiles revealed dysregulation of several inflammatory genes in frontal cortex of CDS-suffering animals compared with normally aged dogs. We found significant upregulation of chemokine CCL2 (2.42-fold) and interleukin (IL) 1A (1.48-fold), together with increased expression of IL1R1 (1.44-fold), adhesion molecule ICAM1 (1.35-fold), and CD28 (2.02-fold). Furthermore, we identified elevated expression of genes associated with toll-like receptor pathways such as TLR5 (1.45-fold) and LY96 (1.58-fold). Upregulation of genes involved in apoptosis CASP4 (1.50-fold) and protection against reactive oxygen species in macrophages SLC11A1 (1.26-fold) was also observed (Fig. 6). Complete transcriptomic data including other nonsignificantly dysregulated genes are listed in Table 3.

### Cognitive impairment in dogs is associated with increase in tau phosphorylation in the synaptic terminals

In total six nondemented dogs and six demented dogs based on DISHA scoring (Osella et al., 2007) were used for the study of a subset of synaptic proteome. For consistency, three separate isolations of synaptosomes were performed from all samples. Western blotting of synaptosomes isolated from prefrontal cortex revealed that the levels of tau protein were significantly elevated in the synapses of demented dogs in comparison with nondemented dogs ( $P = 0.013$ ; Fig. 7A,B). Similarly, we found upregulation of the postsynaptic protein drebrin ( $P = 0.013$ ). Two other tested synaptic proteins, synaptophysin ( $P = 0.7$ ) and GAP43 ( $P = 0.308$ ), did not show any significant differences between demented and nondemented dogs (Fig. 7A,B).

We then focused on site-specific phosphorylation of tau protein, which is associated with pathological conditions in AD (Augustinack et al., 2002). We analyzed tau phospho-sites relevant for AD, such as pS199, pT205, pT212, pS214, and pS404. Antibodies specifically targeting these phospho-sites were used to evaluate the changes in tau phosphorylation levels in demented canine brains. Sarkosyl-insoluble fraction from an AD brain was used as a positive control for staining of antibodies. The levels of phospho-tau and total tau (polyclonal tau antibody) were normalized to actin, and the ratio between phospho-tau and total tau was calculated. Tau protein in demented dogs showed increased phosphorylation at residues S199 ( $P = 0.01$ ), T205 ( $P = 0.003$ ), T212

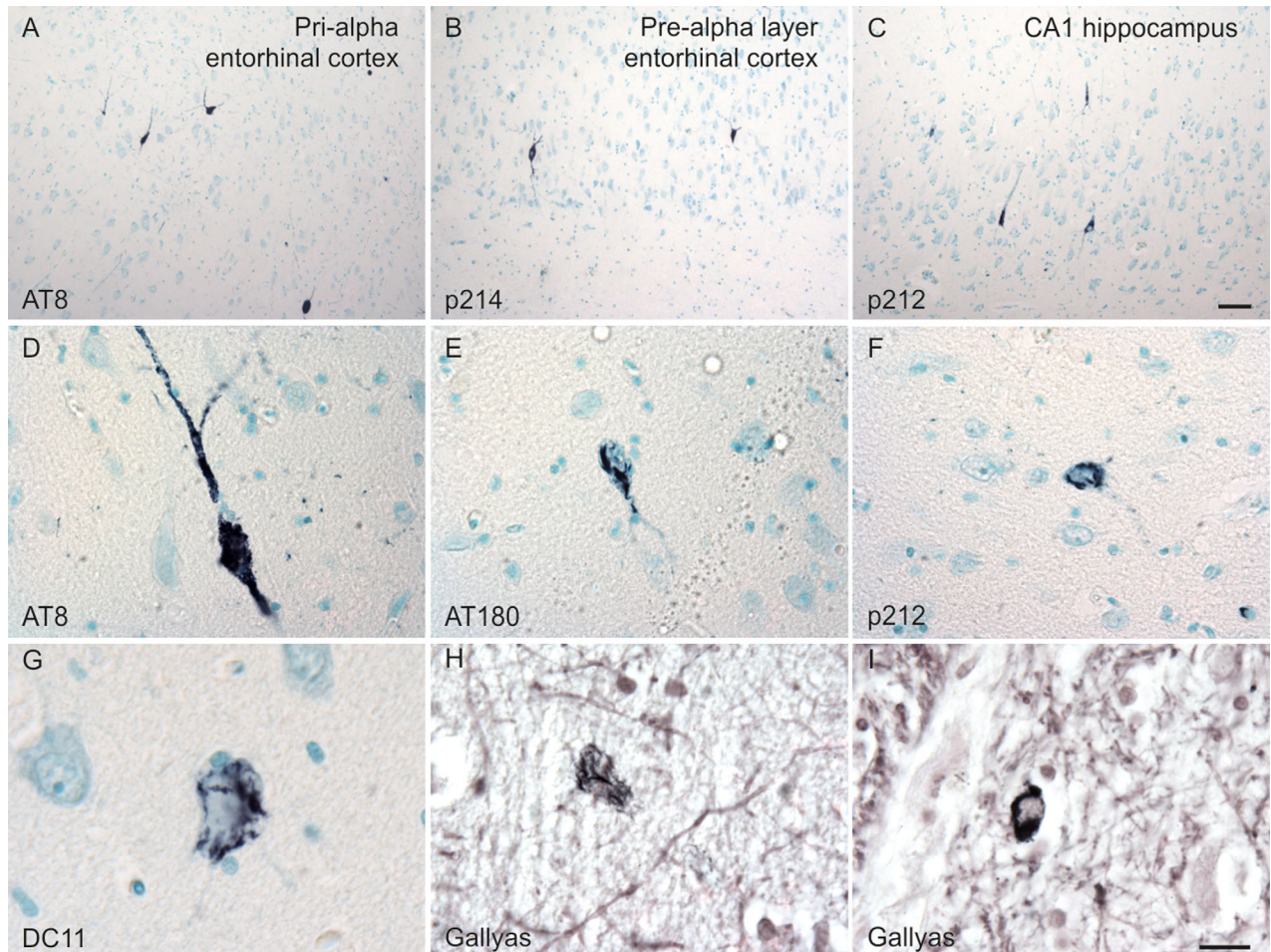


**Figure 3.** Tau neurofibrillary structures in a demented, aged Pekingese. For one 13-year-old Pekingese suffering from dementia, we identified fibrillary structures in several brain areas, including Pri- $\alpha$  layer (A) and Pre- $\alpha$  layer (B) of entorhinal cortex and CA1 sector of the hippocampus (C). Higher magnification showed the presence of fibrillary structures inside neurons immunolabeled with anti-tau antibodies AT8 (D), AT180 (E), pT212 (F), and DC11 (G). Some fibrillary structures were positive for Gallyas silver staining (H,I). Scale bars = 100  $\mu$ m in C (applies to A–C); 20  $\mu$ m in H (applies to D–H).

( $P = 0.002$ ), S214 ( $P = 0.002$ ), and S404 ( $P = 0.013$ ; Fig. 7C,D). Finally, we performed a correlation study to analyse the relationship between the level of clinical impairment and the tau phosphorylation in synapses. The study revealed that there was a positive correlation between DISHA score and tau phosphorylation at pT205 (Fig. 7E;  $r = 0.445$ ,  $P < 0.001$ ) or pS214 (Fig. 7F;  $r = 0.425$ ,  $P < 0.01$ ).

To determine whether these changes in tau synaptic proteome are brain area specific, we analyzed four selected areas, frontal and temporal cortices, hippocampus, and cerebellum. We observed that synaptic tau protein levels were similar in all selected brain regions ( $P = 0.134$ ; Fig. 8A,B). However, the level of tau phosphorylation in synaptosomes, represented by phospho-tau (pT205) to total tau ratio, was increased in the frontal cortex but not in the other brain areas analyzed ( $P = 0.001$ ; Fig. 8A,C).

## DISCUSSION

Canine cognitive decline represents a group of symptoms related to the aging of the canine brain. The disease is characterized by deposition of  $\beta$ -amyloid protein in cerebral cortex vascular amyloid angiopathy, astrogliosis, and neuronal loss (Borras et al., 1999). In dogs, the accumulation of  $\beta$ -amyloid plaques is an age-dependent process starting in the prefrontal cortex and spreading with increasing age to other regions such as the temporal and occipital cortex (Russell et al., 1996). Previous studies demonstrated that the extent of  $\beta$ -amyloid deposition correlates with cognitive decline (Cummings et al., 1996; Head et al., 1998; Colle et al., 2000; Rofina et al., 2006; Pugliese et al., 2006). Our results show that  $\beta$ -amyloid deposition can be used for discrimination between cognitively normal and demented dogs. However, in terms of plaque density in demented dogs' brains, we observed great interindividual variability, and

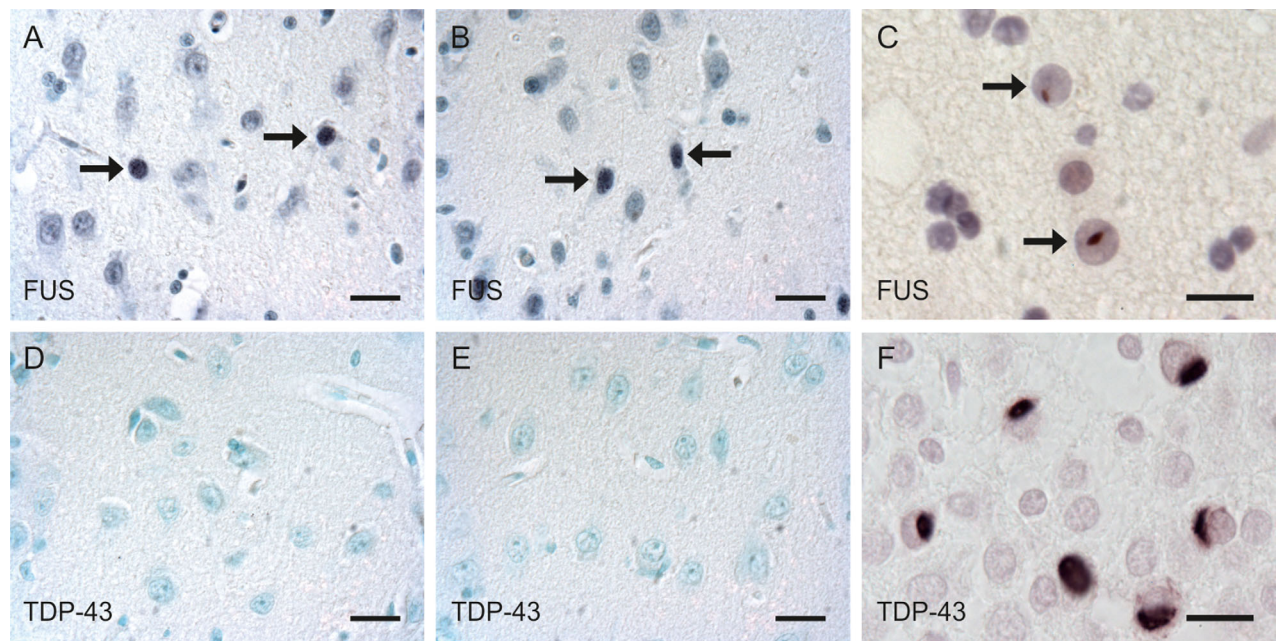


**Figure 4.** The absence of TDP43 and FUS aggregates in canine brain. Anti-FUS antibody recognized small intranuclear dots in frontal (A) and temporal (B) cortices. Human brain sample from FUS-positive FTLD case was used as a control (C). Anti-TDP43 antibody did not show any pathological lesions in either frontal (D) or temporal (E) cortex. Human brain sample from TDP43-positive FTLD case was used as a control (F). Scale bars = 20  $\mu$ m.

the density did not reflect the DISHA score. Czasch et al. (2006) found the presence of several subgroups of dogs according to the number of detectable plaques. He suggested that this might indicate breed differences in susceptibility to age-related neuropathology.

Unlike human plaques, canine amyloid plaques do not contain activated microglia. Our findings are in accordance with previously published data showing that most plaques did not contain glial cells (Uchida et al., 1993; Rofina et al., 2003). On the other hand, for many demented dogs we observed activated and dystrophic microglia. Previously, Hwang et al. (2008) showed Iba1-immunoreactive hypertrophic microglia with bulbous swelling processes in the dentate gyrus and CA1 region of the aged dog. As seen in human aging (Streit, 2006), canine microglial cells are characterized by abnormalities in their cytoplasmic structure, such as deramified, fragmented, or tortuous processes, occasionally bearing spheroidal or bulbous swellings.

The most striking feature of the aged dog brain, however, is the presence of microglial clusters. Wolfgang Streit demonstrated that human microglia in aged brain may lose contact inhibition and begin to fuse with each other. This fusion can lead to the formation of microglial clusters consisting of three or even more cells (Streit et al., 1999). Our findings are in line with observations in the human brain; in many aged dog brains

we observed microglial clusters containing either hypertrophic ramified cells or deramified reactive cells. There is no relationship between plaque density or distribution and microglial clusters suggesting that they represent independent disease processes. We conclude that activated and dystrophic microglia represent a consistent feature of the brain of demented dogs. It is important to note that there is a great variation in distribution of dystrophic microglia in individual dogs. Some demented dogs did not show any sign of microglia immunosenescence. Transcriptomic data suggest that peripheral immune system may take part in the disease process as well. The presence of at least two upregulated genes in the brain, CD28 and lymphocyte antigen 96, indicates the presence of lymphocytes in the affected brain. This notion further substantiates the upregulation of genes coding chemokine CCL2 and ICAM 1 that are involved in the trafficking of leukocytes through the blood-brain barrier. Further studies are warranted to unravel the contribution of peripheral lymphocytes on the pathogenesis of CDS.

A characteristic feature of the aged canine brain is the atrophy of frontal and temporal cortex (Tapp et al., 2004). The frontal cortex also represents the starting point of  $\beta$ -amyloid pathology (Russell et al., 1996). These findings indicate that frontal cortex is the main vulnerable brain area in canine dementia. In humans,

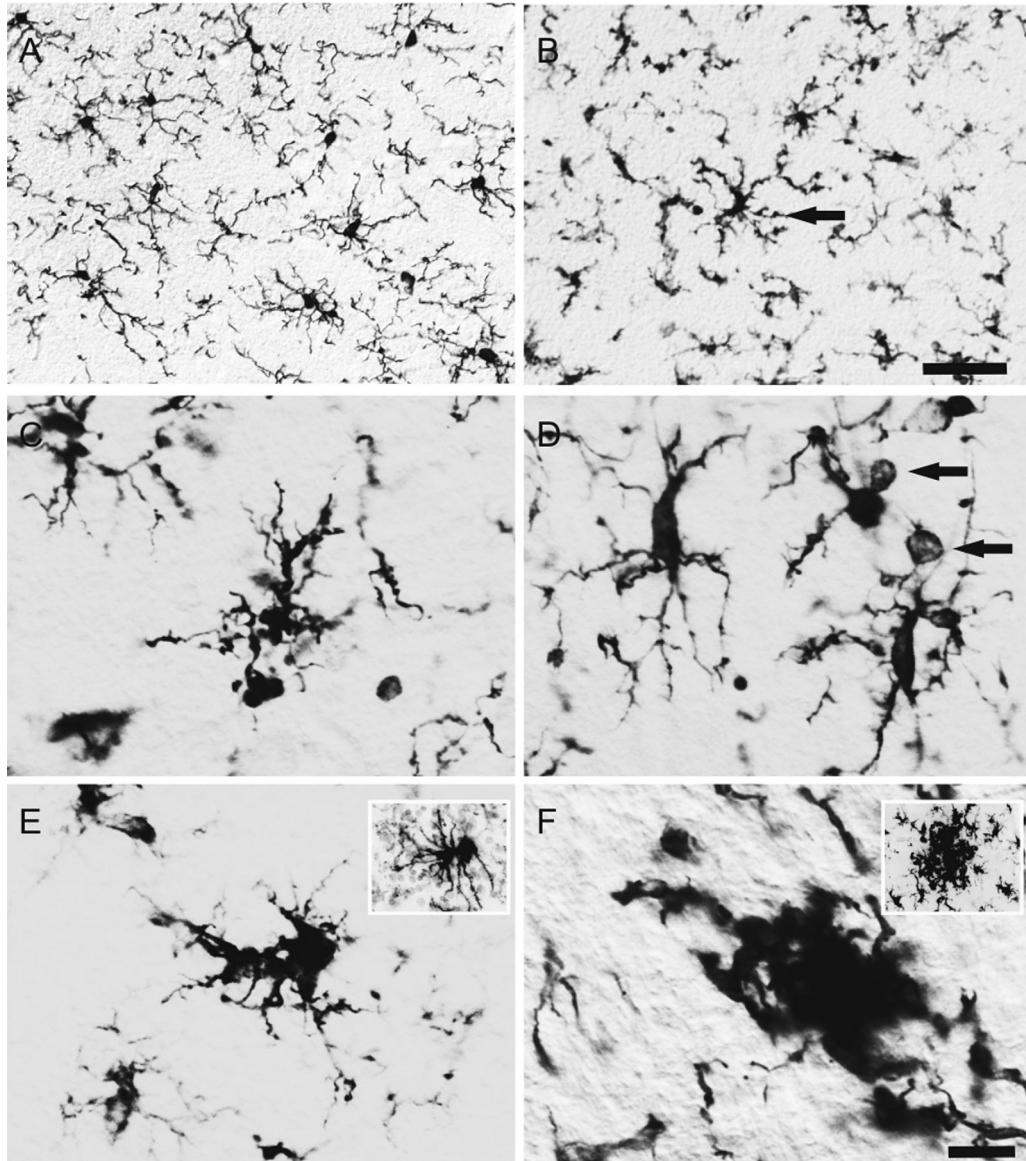


**Figure 5.** Dystrophic and clustered microglia in demented canine brain. In nondemented dogs, predominantly resting microglial cells are distributed in the hippocampus (A). In demented dogs, activated (arrow) or dystrophic forms of microglia are present (B). In demented dogs, traces of brain immunosenescence were present in the form of microglial cells with fragmented processes (C) and dystrophic microglia with spheroidal or bulbous swellings (D; arrows). Microglial clusters represent another important feature of the aged dog brain. Early microglial clusters contained ramified activated microglial cells (E), whereas late microglial clusters consisted mostly of reactive microglia with short, deramified processes (F). **Insets** show higher magnifications of clustered microglia in human AD brains. Scale bars = 100  $\mu$ m in B (applies to A,B); 20  $\mu$ m in F (applies to C-F).

primarily the frontal and temporal cortices are affected by neurodegeneration in FTLD. Three major proteins have been identified as driving forces behind neurodegeneration characteristic for FTLD; the tau protein, TDP43, and FUS (Josephs et al., 2011). Here we investigated whether these three protein candidates might participate in neurodegeneration in canine dementia.

The intraneuronal accumulation of hyperphosphorylated tau has been reported for brains of dogs and other mammalian species such as monkeys, bison,

rabbits, reindeer, wolverines, bears, goats, sheep, and cats. Most affected neurons have been identified as pyramidal neurons (Cork et al., 1988; Braak et al., 1994; Nelson et al., 1994; Roertgen et al., 1996; Hartig et al., 2000; Head et al., 2005; Gunn-Moore et al., 2006). Two studies demonstrated wide distribution of tau protein phosphorylated on Ser396 in neurons and astrocytes in the canine brain; however, the signal was rather diffuse, and fibrillar structures were absent (Pugliese et al., 2006; Yu et al., 2011). Here we show

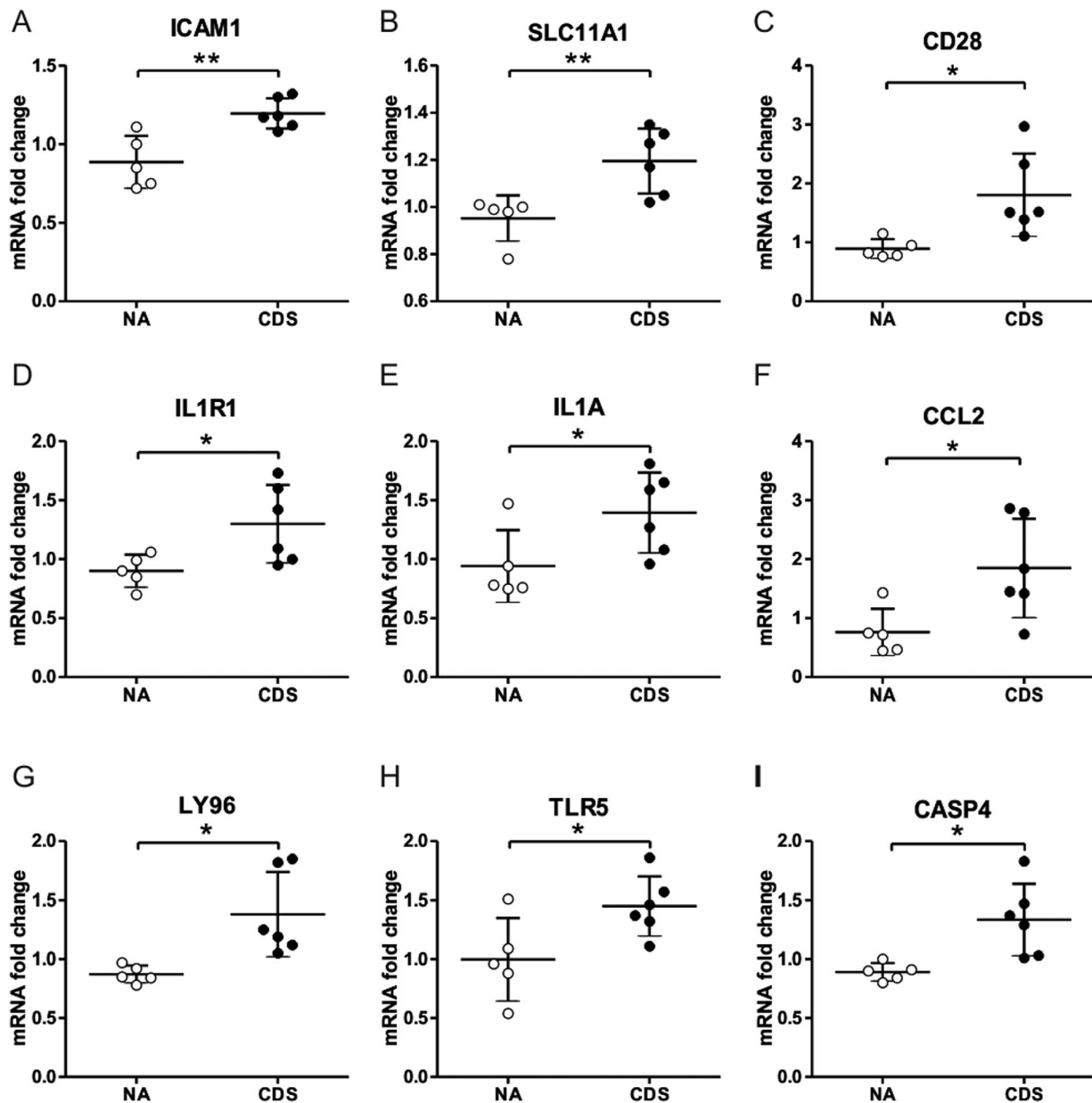


**Figure 6.** CDS animals display elevated expression of inflammatory genes in frontal cortex. Transcriptomic analysis revealed upregulation of cell adhesion molecule ICAM1 (A), macrophage SLC11A1 (B), and T-cell receptor costimulatory molecule CD28 (C) in CDS animals. Increased expression of interleukin 1 receptor type 1 (D) and its ligand IL1A (E) together with chemokine CCL2 was also identified in CDS animals compared with normal aging (NA) controls. Elevation of genes involved in toll-like receptor signaling LY96 (G), TLR5 receptor (H), and upregulation of inflammation-related caspase 4 (I) was also observed in frontal cortex of CDS animals. Differences between normal aging and CDS groups were considered statistically significant at  $*P < 0.05$  and  $**P < 0.01$  (NA  $n = 5$ , CDS  $n = 6$ ).

that at least in some dog breeds tau fibrillar structure containing hyperphosphorylated and conformationally modified tau protein can be present in hippocampus and cortex as well.

Until now, argyrophilic NFTs and NTs have not been documented in dogs. The presence of argyrophilic NFTs in the brains of aged dogs was mentioned only once by Papaioannou et al. (2001), but the authors did not present any data supporting this claim. The lack of NFT

pathology was explained by significant differences in the tau protein sequence between dogs and humans (Davis and Head, 2014). Recently, we found that the key structural determinants essential for pathological tau-tau interaction were located inside the microtubular binding domains (MBD; Kontseikova et al., 2014). The protein sequences of tau MBD in humans and dogs share 99% sequence homology. This study demonstrates that dog can develop argyrophilic tau fibrillary

**TABLE 3.**  
Gene Expression Profile of Innate and Adaptive Immune Response-Related Genes in Demented Dogs<sup>1</sup>

Gene symbol	Gene specifically altered	Relative quantity		Fold change	P value
		NA	CDS	CDS/NA	
<i>CASP4</i>	Caspase 4, apoptosis-related cysteine peptidase	0.89	1.33	1.50	0.0147
<i>CCL2</i>	Chemokine (C-C motif) ligand 2	0.76	1.85	2.42	0.0248
<i>CD28</i>	CD28 molecule	0.89	1.81	2.02	0.0227
<i>ICAM1</i>	Intercellular adhesion molecule 1	0.89	1.20	1.35	0.0099
<i>IL1A</i>	Interleukin 1 alpha	0.94	1.40	1.48	0.0440
<i>IL1R1</i>	Interleukin 1 receptor, type I	0.90	1.30	1.44	0.0310
<i>LY96</i>	Lymphocyte antigen 96	0.87	1.38	1.58	0.0169
<i>SLC11A1</i>	Solute carrier family 11 (proton-coupled divalent metal ion transporter) member 1	0.95	1.19	1.26	0.0078
<i>TLR5</i>	Toll-like receptor 5	0.99	1.45	1.45	0.0483
<i>APCS</i>	Amyloid P component, serum	0.88	0.59	0.67	0.2252
<i>C3</i>	Complement component 3	1.08	1.28	1.19	0.3959
<i>C5AR1</i>	Complement component 5a receptor 1	0.94	0.93	0.99	0.9480
<i>CAMP</i>	Cathelicidin antimicrobial peptide	0.45	1.20	2.64	0.3141
<i>CCL3</i>	Chemokine (C-C motif) ligand 3	0.99	1.30	1.32	0.1104
<i>CCL5</i>	Chemokine (C-C motif) ligand 5	1.08	1.48	1.37	0.3778
<i>CCR4</i>	Chemokine (C-C motif) receptor 4	0.99	1.38	1.38	0.3209
<i>CCR5</i>	Chemokine (C-C motif) receptor 5	1.01	1.19	1.18	0.3229
<i>CCR6</i>	Chemokine (C-C motif) receptor 6	1.19	0.80	0.67	0.2497
<i>CCR8</i>	Chemokine (C-C motif) receptor 8	1.49	0.87	0.59	0.2616
<i>CD14</i>	CD14 molecule	1.01	1.00	0.99	0.9151
<i>CD1A6</i>	CD1a6 molecule	0.65	0.89	1.37	0.3159
<i>CD209</i>	CD209 molecule	1.16	1.07	0.92	0.8303
<i>CD4</i>	CD4 molecule	0.85	1.33	1.56	0.0672
<i>CD40</i>	CD40 molecule	1.06	1.20	1.13	0.4858
<i>CD40LG</i>	CD40 Ligand	1.00	1.10	1.09	0.4789
<i>CD80</i>	CD80 molecule	1.01	1.04	1.03	0.8722
<i>CD86</i>	CD86 molecule	0.99	1.15	1.15	0.2993
<i>CD8A</i>	CD8a molecule	0.99	1.83	1.85	0.1823
<i>CRP</i>	C-reactive protein	1.23	2.92	2.38	0.1108
<i>CSF2</i>	Colony-stimulating factor 2	1.17	1.77	1.51	0.2117
<i>CXCL10</i>	Chemokine (C-X-C motif) ligand 10	1.24	1.27	1.02	0.9602
<i>CXCR3</i>	Chemokine (C-X-C motif) receptor 3	1.09	1.89	1.74	0.1903
<i>FASLG</i>	Fas ligand (TNF superfamily member 6)	1.03	1.44	1.39	0.2549
<i>FOXP3</i>	Forkhead box P3	1.01	0.97	0.96	0.6528
<i>GATA3</i>	GATA binding protein 3	1.06	0.89	0.84	0.6017
<i>IFNB1</i>	Interferon beta 1	1.12	1.33	1.19	0.6613
<i>IFNG</i>	Interferon gamma	1.61	2.06	1.27	0.7089
<i>IL10</i>	Interleukin 10	1.03	1.46	1.41	0.0764
<i>IL13</i>	Interleukin 13	1.05	1.27	1.21	0.3440
<i>IL15</i>	Interleukin 15	0.98	1.01	1.04	0.7245
<i>IL17A</i>	Interleukin 17A	nd	nd	nd	nd
<i>IL18</i>	Interleukin 18	0.95	1.30	1.37	0.1207
<i>IL1B</i>	Interleukin 1 beta	1.11	1.71	1.54	0.4343
<i>IL2</i>	Interleukin 2	1.91	2.71	1.42	0.4765
<i>IL4</i>	Interleukin 4	1.04	1.28	1.23	0.1266
<i>IL5</i>	Interleukin 5	0.97	1.02	1.05	0.7444
<i>IL6</i>	Interleukin 6	1.04	0.99	0.95	0.7838
<i>IL8</i>	Interleukin 8	0.70	1.97	2.81	0.3321
<i>IRAK1</i>	Interleukin-1 receptor-associated kinase 1	1.02	1.01	0.99	0.9321
<i>IRF3</i>	Interferon regulatory factor 3	1.03	1.03	1.01	0.9531
<i>IRF6</i>	Interferon regulatory factor 6	1.00	1.23	1.23	0.1942
<i>ITGAM</i>	Integrin, alpha M (complement component 3 receptor 3 subunit)	0.99	0.89	0.90	0.5924
<i>JAK2</i>	Janus kinase 2	1.03	1.06	1.03	0.6141
<i>LBP</i>	Lipopolysaccharide binding protein	1.01	1.52	1.50	0.1221
<i>LYZ</i>	Lysozyme	0.93	0.83	0.89	0.7184
<i>MAPK1</i>	Mitogen-activated protein kinase 1	1.03	0.97	0.94	0.5079
<i>MAPK8</i>	Mitogen-activated protein kinase 8	1.03	0.91	0.89	0.0958
<i>MPO</i>	Myeloperoxidase	1.11	1.15	1.04	0.8457

TABLE 3. Continued

Gene symbol	Gene specifically altered	Relative quantity		Fold change	P value
		NA	CDS	CDS/NA	
MX1	Myxovirus (influenza virus) resistance 1, interferon-inducible protein p78 (mouse)	1.03	0.87	0.85	0.1271
MYD88	Myeloid differentiation primary response 88	0.97	0.97	1.00	0.9663
NFKB1	Nuclear factor kappa B1	1.01	1.02	1.01	0.9251
NFKBIA	Nuclear factor kappa B1A	1.08	1.16	1.08	0.7419
NLRP3	NLR family, pyrin domain containing 3	0.98	1.23	1.26	0.3027
NOD1	Nucleotide-binding oligomerization domain containing 1	1.01	1.11	1.10	0.3326
NOD2	Nucleotide-binding oligomerization domain containing 2	1.06	1.31	1.24	0.3030
RAG1	Recombination-activating gene 1	1.03	0.79	0.76	0.2717
RORC	RAR-related orphan receptor C	0.99	1.20	1.21	0.3844
STAT1	Signal transducer and activator of transcription 1	1.04	0.96	0.92	0.3861
STAT3	Signal transducer and activator of transcription 3	0.97	1.06	1.10	0.2146
STAT4	Signal transducer and activator of transcription 4	1.07	1.10	1.03	0.8387
STAT6	Signal transducer and activator of transcription 6	1.00	0.93	0.93	0.4207
TBX21	T-box 21	0.82	1.09	1.34	0.5533
TICAM1	Toll-like receptor adaptor molecule 1	0.95	1.16	1.22	0.1109
TLR1	Toll like receptor 1	0.99	1.09	1.10	0.6078
TLR2	Toll like receptor 2	1.06	1.57	1.48	0.3324
TLR3	Toll like receptor 3	0.99	1.11	1.12	0.3446
TLR4	Toll like receptor 4	0.94	1.10	1.17	0.1437
TLR6	Toll like receptor 6	1.01	0.88	0.87	0.2374
TLR7	Toll like receptor 7	1.03	1.01	0.98	0.9282
TLR8	Toll like receptor 8	1.22	2.48	2.03	0.3471
TLR9	Toll like receptor 9	1.02	1.53	1.50	0.2018
TNF	Tumor necrosis factor	0.95	1.29	1.36	0.3071
TRAF6	TNF receptor-associated factor 6	1.03	1.00	0.98	0.7579
TYK2	Tyrosine kinase 2	1.00	1.14	1.15	0.1995

<sup>1</sup>Genes in italics represent significantly upregulated genes.

structures, suggesting that canine brain is partially vulnerable to neurofibrillary degeneration.

We then focused on the other two protein candidates responsible for neurodegeneration in human FTL, namely, FUS and TDP43. We performed an extensive screening of 20 demented dogs focusing on frontal and temporal cortex (including hippocampus). We did not find any pathological aggregates, suggesting that canine brain is not vulnerable for FUS and TDP43 neurodegeneration. These data suggest that neurodegeneration characteristic for human FTL is not present in canine brain, neither in very old dogs nor in dogs suffering from severe cognitive impairment. This finding further substantiates the idea that canine cognitive impairment does not represent human-like neurodegenerative disorder characterized by specific neuronal or glial aggregates.

Synaptic deficits correlate well with the severity of dementia in human Alzheimer's disease patients (Masliah et al., 2001; Scheff et al., 2007). The synaptic damage is characterized by deregulation of synaptic proteins at the protein and mRNA levels (Coleman and Yao, 2003; Honer, 2003). We and others have shown that phosphorylated, mutated, and truncated forms of

tau protein play an important role in the synaptic damage (Warmus et al., 2014; Jadhav et al., 2015). Synaptic accumulation of phosphorylated tau was observed in AD (Tai et al., 2012; Tai et al., 2014), mainly in the frontal cortex (Herrmann et al., 1999). Similar to human AD, synaptosomes of demented dogs contained substantial accumulation of total tau protein along with hyperphosphorylation at residues S199, T205, T212, S214, and S404. We showed previously in a rat model of human tauopathy that tau phosphorylated at T205, S214, and S404 was enriched in the postsynaptic compartment, whereas *P*-tau T212 was increased mainly in the presynaptic compartment together with concomitant decrease in drebrin protein levels (Jadhav et al., 2015). The abnormal accumulation of tau in dogs was associated with selective deregulation of synaptic proteome. Although synaptophysin and GAP43 did not show any significant changes, we observed an increase in drebrin in demented dogs. Drebrin is a filamentous actin-binding protein involved in dendritic plasticity and receptor targeting to synapses (Majoul et al., 2007). Increased levels of drebrin were shown in the frontal cortex of patients with mild

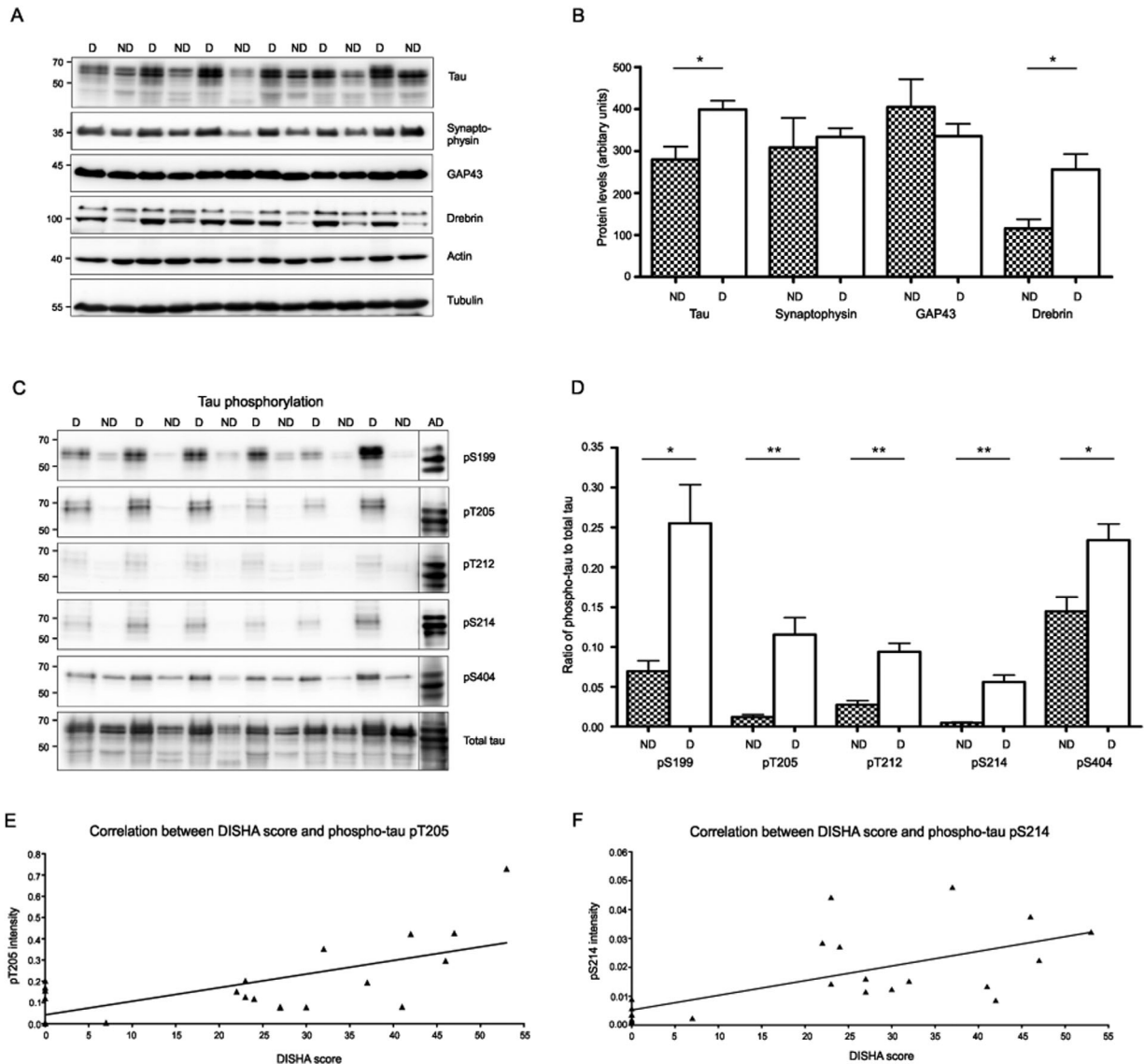


**Figure 7.** Abnormal hyperphosphorylation of synaptic tau in frontal cortex of demented dogs. **A:** Western blots of selected proteins from synaptosomal fractions isolated from brains of demented (D) and nondemented (ND) dogs ( $n = 6/\text{group}$ ). Actin and tubulin were used as loading controls. **B:** Bar graphs showing levels of selected proteins. Statistical analysis revealed significant increase in tau and drebrin. All values were normalized to actin. **C:** Immunoblots of total and phospho-tau in synaptosomal fractions from demented and nondemented dogs. **D:** Bar graph showing intensity levels of phospho-tau in the two groups. Levels of phospho-tau were normalized to total tau levels. Statistical analysis revealed a significant increase in all the phospho-tau epitopes analyzed. Correlations between modified DISHA score and phospho-tau levels in synapses stained by antibodies pT205 (**E**) and pS214 (**F**). Graphs represent mean  $\pm$  SEM. \* $P < 0.05$ , \*\* $P < 0.01$ .

cognitive impairment and AD (Counts et al., 2006; Leuba et al., 2008a,b). The increase in drebrin may be considered as compensatory mechanism for synaptic impairment in the dogs exhibiting clinical signs of cognitive decline. However, alterations in synaptic protein levels may or may not suggest changes in synapse number or increase in synapse density but might rather reflect changes in synaptic function (Head et al., 2009).

To determine whether increased tau phosphorylation in synapses is brain area specific, we compared the levels of total tau and phospho-tau in four selected brain areas, frontal and temporal cortices, hippocampus, and cerebellum. Tau phosphorylation was elevated in frontal cortex only, which reflects selective vulnerability of this brain area to canine brain aging. This is in accordance with other studies showing that prefrontal cortex is considered to be the earliest and more consistently

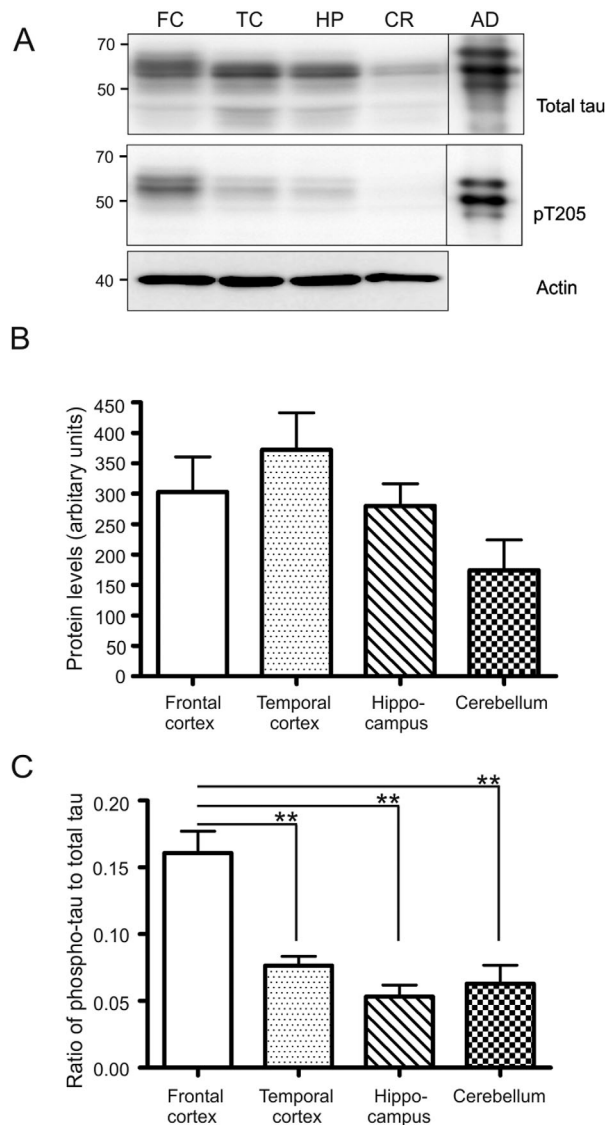


**Figure 8.** Hyperphosphorylation of synaptic tau is characteristic for frontal cortex. **A:** Immunoblots of total and phospho-tau (T205) from synaptosomal fractions isolated from frontal cortex (FC), temporal cortex (TC), hippocampus (HP), and cerebellum (CR). **B:** Graph showing levels of tau protein in the brain regions analyzed. No significant differences in tau protein expression were seen in selected brain areas. **C:** Graph showing intensities of phospho-tau T205 in brain areas studied. Statistical analysis revealed higher amounts of phospho-tau T205 in the frontal cortex compared with other brain areas. Graphs represent mean  $\pm$  SEM.  $**P < 0.01$ .

affected brain area in canine cognitive decline (Yoshino et al., 1996; Hou et al., 1997; Head et al. 2000). Moreover, it is important to note that similar elevation was found also in frontal cortex of AD brain (Herrmann et al., 1999; Causevic et al., 2010), suggesting an identical pattern of synaptic tau abnormalities in human and canine brain.

Here we have demonstrated that synaptic impairment rather than classic human-like neurodegeneration represents the molecular substrate of canine cognitive impairment. This may open new vistas for development of new diagnostic and therapeutic approaches for canine dementia.

## ACKNOWLEDGMENTS

We thank Tomas Hromadka, who performed the statistical analysis of the data. The authors are grateful to Prof. Dr. Irina Alafuzoff, Prof. Constantin Bouras, and Prof. Eniko Kovari for the outstanding practical advice on human brain neuropathology.

## CONFLICT OF INTEREST STATEMENT

The authors declare that they have no conflict of interest.

## ROLE OF AUTHORS

Study design: AM, NZ, MN. Acquisition of data: AM, JF, TS, VB, SJ, PN. Analysis and interpretation of data: NZ, AM, TS, MN, PN. Article draft: NZ, AM, MN, PN.

## LITERATURE CITED

- Alafuzoff I, Arzberger T, Al-Sarraj S, Bodi I, Bogdanovic N, Braak H, Bugiani O, Del-Tredici K, et al. 2008. Staging of neurofibrillary pathology in Alzheimer's disease: a study of the BrainNet Europe Consortium. *Brain Pathol* 18: 484-496.
- Augustinack JC, Schneider A, Mandelkow EM, Hyman BT. 2002. Specific tau phosphorylation sites correlate with severity of neuronal cytopathology in Alzheimer's disease. *Acta Neuropathol* 103:26-35.
- Ball MJ, MacGregor J, Fyfe IM, Rapoport SI, London ED. 1983. Paucity of morphological changes in the brains of ageing beagle dogs: further evidence that Alzheimer lesions are unique for primate central nervous system. *Neurobiol Aging* 4:127-131.
- Benjamini Y, Hochberg Y. 1995. Controlling the false discovery rate: a practical and powerful approach to multiple testing. *J R Statist Soc Ser B* 57:289-300.
- Borras D, Ferrer I, Pumarola M. 1999. Age-related changes in the brain of the dog. *Vet Pathol* 36:202-211.
- Braak H, Braak E, Strothjohann M. 1994. Abnormally phosphorylated tau protein related to the formation of neurofibrillary tangles and neurophil threads in the cerebral cortex of sheep and goat. *Neurosci Lett* 171:1-4.
- Causevic M, Farooq U, Lovestone S, Killick R. 2010.  $\beta$ -Amyloid precursor protein and tau protein levels are differently regulated in human cerebellum compared to brain regions vulnerable to Alzheimer's type neurodegeneration. *Neurosci Lett* 485:162-166.
- Chang RY, Nouwens AS, Dodd PR, Etheridge N. 2013. The synaptic proteome in Alzheimer's disease. *Alzheimers Dement* 9:499-511.
- Cohen RS, Blomberg F, Berzins K, Siekevitz P. 1977. The structure of postsynaptic densities isolated from dog cerebral cortex. I. Overall morphology and protein composition. *J Cell Biol* 74:181-203.

- Coleman PD, Yao PJ. 2003. Synaptic slaughter in Alzheimer's disease. *Neurobiol Aging* 24:1023–1027.
- Colle MA, Hauw JJ, Crespeau F, Uchihara T, Akiyama H, Checler F, Pageat P, Duykaerts C. 2000. Vascular and parenchymal Abeta deposition in the aging dog: correlation with behavior. *Neurobiol Aging* 21:695–704.
- Cork LC, Powers RE, Selkoe DJ, Davies P, Geyer JJ, Price DL. 1988. Neurofibrillary tangles and senile plaques in aged bears. *J Neuropathol Exp Neurol* 7:629–641.
- Cotman CW, Head E. 2011. The canine model of human aging and disease. In: Casadesus G, editor, *Handbook of animal models in Alzheimer's disease*. Amsterdam: IOS Press. p 15–38.
- Counts SE, Nadeem M, Lad SP, Wu J, Mufson EJ. 2006. Differential expression of synaptic proteins in the frontal and temporal cortex of elderly subjects with mild cognitive impairment. *J Neuropathol Exp Neurol* 65:592–601.
- Cummings BJ, Head E, Ruehl W, Milgram NW, Cotman CW. 1996. The canine as an animal model of human aging and dementia. *Neurobiol Aging* 17:259–268.
- Czasch S, Paul S, Baumgärtner W. 2006. A comparison of immunohistochemical and silver staining methods for the detection of diffuse plaques in the aged canine brain. *Neurobiol Aging* 27:293–305.
- Davis PR, Head E. 2014. Prevention approaches in a preclinical canine model of Alzheimer's disease: benefits and challenges. *Front Pharmacol* 21:5:47.
- Efron B, Tibshirani RJ. 1993. *An introduction to the bootstrap*, 1st ed. New York: Chapman and Hall.
- Filipczik P, Zilka N, Bugos O, Kucerak J, Koson P, Novak P, Novak M. 2012. First transgenic rat model developing progressive cortical neurofibrillary tangles. *Neurobiol Aging* 33:1448–1456.
- Fontana F1, Siva K1, Denti MA. 2015. A network of RNA and protein interactions in frontotemporal dementia. *Front Mol Neurosci* 8:9.
- Gallyas F. 1971. Silver staining of Alzheimer's neurofibrillary changes by means of physical development. *Acta Morphol Acad Sci Hung* 19:1–8.
- Giaccone G, Verga L, Finazzi M, Polio B, Tagliavini F, Frangione B, Bugiani O. 1990. Cerebral preamyloid deposits and congophilic angiopathy in aged dogs. *Neurosci Lett* 114:178–183.
- González-Soriano J, Marín García P, Contreras-Rodríguez J, Martínez-Sainz P, Rodríguez-Veiga E. 2001. Age-related changes in the ventricular system of the dog brain. *Ann Anat* 183:283–291.
- Gunn-Moore DA, McVee J, Bradshaw JM, Pearson GR, Head E, Gunn-Moore FJ. 2006. Ageing changes in cat brains demonstrated by beta-amyloid and AT8-immunoreactive phosphorylated tau deposits. *J Feline Med Surg* 8:234–242.
- Hartig W, Klein C, Brauer K, Schuppel KF, Arendt T, Bruckner G, et al. 2000. Abnormally phosphorylated protein tau in the cortex of aged individuals of various mammalian orders. *Acta Neuropathol* 100:305–312.
- Head E, Callahan H, Muggenburg BA, Cotman CW, Milgram NW. 1998. Visual-discrimination learning ability and beta-amyloid accumulation in the dog. *Neurobiol Aging* 19:415–425.
- Head E, McCleary R, Hahn FF, Milgram NW, Cotman CW. 2000. Region specific age at onset of beta-amyloid in dogs. *Neurobiol Aging* 21:89–96.
- Head E, Moffat K, Das P, Sarsoza F, Poon WW, Landsberg G, Cotman CW, Murphy MP. 2005. Beta-amyloid deposition and tau phosphorylation in clinically characterized aged cats. *Neurobiol Aging* 26:749–763.
- Head E, Corrada MM, Kahle-Wroblewski K, Kim RC, Sarsoza F, Goodus M, Kawas CH. 2009. Synaptic proteins, neuropathology and cognitive status in the oldest-old. *Neurobiol Aging* 30:1125–1134.
- Herrmann M, Golombowski S, Kräuchi K, Frey P, Mourton-Gilles C, Hulette C, Rosenberg C, Müller-Spahn F, Hock C. 1999. ELISA-quantitation of phosphorylated tau protein in the Alzheimer's disease brain. *Eur Neurol* 42:205–210.
- Honer WG. 2003. Pathology of presynaptic proteins in Alzheimer's disease: more than simple loss of terminals. *Neurobiol Aging* 24:1047–1062.
- Hou Y, White RG, Bobik M, Marks JS and Russell MJ. 1997. Distribution of beta-amyloid in the canine brain. *Neuroreport* 8:1009–1012.
- Hwang IK, Lee CH, Li H, Yoo KY, Choi JH, Kim DW, Kim DW, Suh HW, Won MH. 2008. Comparison of ionized calcium-binding adapter molecule 1 immunoreactivity of the hippocampal dentate gyrus and CA1 region in adult and aged dogs. *Neurochem Res* 33:1309–1315.
- Inukai Y, Nonaka T, Arai T, Yoshida M, Hashizume Y, Beach TG, Buratti E, Baralle FE, Akiyama H, Hisanaga S, Hasegawa M. 2008. Abnormal phosphorylation of Ser409/410 of TDP43 in FTLD-U and ALS. *FEBS Lett* 582:2899–2904.
- Jadhav S, Katina S, Kovac A, Kazmerova Z, Novak M, Zilka N. 2015. Truncated tau deregulates synaptic markers in rat model for human tauopathy. *Front Cell Neurosci* 9:24.
- Janke C, Beck M, Stahl T, Holzer M, Brauer K, Bigl V, Arendt T. 1999. Phylogenetic diversity of the expression of the microtubule-associated protein tau: implications for neurodegenerative disorders. *Brain Res Mol Brain Res* 68:119–128.
- Johnstone EM, Chaney MO, Norris FH, Pascual R, Little SP. 1991. Conservation of the sequence of the Alzheimer's disease amyloid peptide in dog, polar bear and five other mammals by cross-species polymerase chain reaction analysis. *Brain Res Mol Brain Res* 10:299–305.
- Josephs KA, Hodges JR, Snowden JS, Mackenzie IR, Neumann M, Mann DM, Dickson DW. 2011. Neuropathological background of phenotypical variability in frontotemporal dementia. *Acta Neuropathol* 122:137–153.
- Kanazawa H, Ohsawa K, Sasaki Y, Kohsaka S, Imai Y. 2002. Macrophage/microglia-specific protein Iba1 enhances membrane ruffling and Rac activation via phospholipase C-gamma-dependent pathway. *J Biol Chem* 277:20026–20032.
- Kontsekova E, Zilka N, Kovacech B, Skrabana R, Novak M. 2014. Identification of structural determinants on tau protein essential for its pathological function: novel therapeutic target for tau immunotherapy in Alzheimer's disease. *Alzheimers Res Ther* 6:45.
- Landsberg G, Araujo JA. 2005. Behavior problems in geriatric pets. *Vet Clin North Am Small Anim Pract* 35:675–698.
- Landsberg GM, Nichol J, Araujo JA. 2012. Cognitive dysfunction syndrome: a disease of canine and feline brain aging. *Vet Clin North Am Small Anim Pract* 42:49–68.
- Leuba G, Savioz A, Vernay A, Carnal B, Kraftsik R, Tardif E, Riederer I, Riederer BM. 2008a. Differential changes in synaptic proteins in the Alzheimer frontal cortex with marked increase in PSD-95 postsynaptic protein. *J Alzheimers Dis* 15:139–151.
- Leuba G, Walzer C, Vernay A, Carnal B, Kraftsik R, Pionton F, Marin P, Bouras C, Savioz A. 2008b. Postsynaptic density protein PSD-95 expression in Alzheimer's disease and okadaic acid induced neuritic retraction. *Neurobiol Dis* 30:408–419.
- Majoul I, Shirao T, Sekino Y, Duden R. 2007. Many faces of drebrin: from building dendritic spines and stabilizing gap

- junctions to shaping neurite-like cell processes. *Histochem Cell Biol* 127:355–361.
- Masliah E, Mallory M, Alford M, DeTeresa R, Hansen LA, McKeel DW Jr, Morris JC. 2001. Altered expression of synaptic proteins occurs early during progression of Alzheimer's disease. *Neurology* 56:127–129.
- Mondragón-Rodríguez S, Trillaud-Doppia E, Dudilot A, Bourgeois C, Lauzon M, et al. 2012. Interaction of endogenous tau protein with synaptic proteins is regulated by N-methyl-D-aspartate receptor-dependent tau phosphorylation. *J Biol Chem* 287:32040–32053.
- Morys J, Narkiewicz O, Maciejewska B, Wegiel J, Wisniewski HM. 1994. Amyloid deposits and loss of neurons in the claustrum of the aged dog. *Neuroreport* 5:1825–1828.
- Nelson PT, Greenberg SG, Saper CB. 1994. Neurofibrillary tangles in the cerebral cortex of sheep. *Neurosci Lett* 170:187–190.
- Neumann M, Rademakers R, Roeber S, Baker M, Kretschmar HA, Mackenzie IR. 2009. A new subtype of frontotemporal lobar degeneration with FUS pathology. *Brain* 132:2922–2931.
- Okuda R, Uchida K, Tateyama S, Yamaguchi R, Nakayama H, Goto N. 1994. The distribution of amyloid beta precursor protein in canine brain. *Acta Neuropathol* 87:161–167.
- Osella MC, Reb G, Odore R, Girardi C, Badino P, Barbero R, Bergamasco L. 2007. Canine cognitive dysfunction syndrome: Prevalence, clinical signs and treatment with a neuroprotective nutraceutical. *Appl Anim Behav Sci* 105:297–310.
- Papaioannou N, Tooten PC, van Ederen AM, Bohl JR, Rofina J, Tsangaris T, et al. 2001. Immunohistochemical investigation of the brain of aged dogs. Detection of neurofibrillary tangles and of 4-hydroxynonenal protein, an oxidative damage product, in senile plaques. *Amyloid* 8:11–21.
- Pugliese M, Carrasco JL, Geloso MC, Mascort J, Michetti F, Mahy N. 2004. Gamma-aminobutyric acidergic interneuron vulnerability to aging in canine prefrontal cortex. *J Neurosci Res* 77:913–920.
- Pugliese M, Mascort J, Mahy N, Ferrer I. 2006. Diffuse beta-amyloid plaques and hyperphosphorylated tau are unrelated processes in aged dogs with behavioral deficits. *Acta Neuropathol* 112:175–183.
- Roertgen KE, Parisi JE, Clark HB, Barnes DL, O'Brien TD, Johnson KH. 1996. Ab-associated cerebral angiopathy and senile plaques with neurofibrillary tangles and cerebral hemorrhage in an aged wolverine (*Gulo gulo*). *Neurobiol Aging* 17:243–247.
- Rofina J, van Andel I, van Ederen AM, Papaioannou N, Yamaguchi H, Gruys E. 2003. Canine counterpart of senile dementia of the Alzheimer type: amyloid plaques near capillaries but lack of spatial relationship with activated microglia and macrophages. *Amyloid* 10:86–96.
- Rofina JE, van Ederen AM, Toussaint MJ, Secrève M, van der Spek A, van der Meer I, Van Eerdenburg FJ, Gruys E. 2006. Cognitive disturbances in old dogs suffering from the canine counterpart of Alzheimer's disease. *Brain Res* 1069:216–226.
- Russell M, White R, Patel E, Markesbery W, Watson C, Geddes J. 1992. Familial influence on plaque formation in the beagle brain. *Neuroreport* 3:1093–1096.
- Russell MJ, Bobik M, White RG, Hou Y, Benjamin SA, Geddes JW. 1996. Age-specific onset of  $\beta$ -amyloid in beagle brains. *Neurobiol Aging* 17:269–273.
- Scheff SW, Price DA, Schmitt FA, DeKosky ST, Mufson EJ. 2007. Synaptic alterations in CA1 in mild Alzheimer disease and mild cognitive impairment. *Neurology* 68:1501–1508.
- Shimada A, Kuwamura M, Umemura T, Takada K, Ohama E, Itakura C, et al. 1991. Bielschowsky and immunohistochemical studies on senile plaques in aged dogs. *Neurosci Lett* 129:25–28.
- Siwak-Tapp CT, Head E, Muggenburg BA, Milgram NW, Cotman CW. 2008. Region specific neuron loss in the aged canine hippocampus is reduced by enrichment. *Neurobiol Aging* 29:39–50.
- Stozicka Z, Zilka N, Novak P, Kovacech B, Bugos O, Novak M. 2010. Genetic background modifies neurodegeneration and neuroinflammation driven by misfolded human tau protein in rat model of tauopathy: implication for immunomodulatory approach to Alzheimer's disease. *J Neuroinflammation* 7:64. doi: 10.1186/1742-2094-7-64.
- Streit WJ. 2006. Microglial senescence: does the brain's immune system have an expiration date? *Trends Neurosci* 29:506–510.
- Streit WJ, Walter SA, Pennell NA. 1999. Reactive microgliosis. *Prog Neurobiol* 57:563–568.
- Streit WJ, Braak H, Xue QS, Bechmann I. 2009. Dystrophic (senescent) rather than activated microglial cells are associated with tau pathology and likely precede neurodegeneration in Alzheimer's disease. *Acta Neuropathol* 118:475–485.
- Tai HC, Serrano-Pozo A, Hashimoto T, Frosch MP, Spires-Jones TL, Hyman BT. 2012. The synaptic accumulation of hyperphosphorylated tau oligomers in Alzheimer disease is associated with dysfunction of the ubiquitin-proteasome system. *Am J Pathol* 181:1426–1435.
- Tai HC, Wang BY, Serrano-Pozo A, Frosch MP, Spires-Jones TL, Hyman BT. 2014. Frequent and symmetric deposition of misfolded tau oligomers within presynaptic and postsynaptic terminals in Alzheimer's disease. *Acta Neuropathol Commun* 2:146.
- Tapp PD, Siwak CT, Gao FQ, Chiou JY, Black SE, Head E, Muggenburg BA, Cotman CW, Milgram NW, Su MY. 2004. Frontal lobe volume, function, and beta-amyloid pathology in a canine model of aging. *J Neurosci* 24:8205–8213.
- Uchida K, Tani Y, Uetsuka K, Nakayama H, Goto N. 1992a. Immunohistochemical studies on canine cerebral amyloid angiopathy and senile plaques. *J Vet Med Sci* 54:659–667.
- Uchida K, Nakayama H, Tateyama S, Goto N. 1992b. Immunohistochemical analysis of constituents of senile plaques and cerebrovascular amyloid in aged dogs. *J Vet Med Sci* 54:1023–1029.
- Uchida K, Okuda R, Yamaguchi R, Tateyama S, Nakayama H, Goto N. 1993. Double-labeling immunohistochemical studies on canine senile plaques and cerebral amyloid angiopathy. *J Vet Med Sci* 55:637–642.
- Vechterova L, Kontseikova E, Zilka N, Ferencik M, Ravid R, Novak M. 2003. DC11: a novel monoclonal antibody revealing Alzheimer's disease-specific tau epitope. *Neuroreport* 14:87–91.
- Wang I, Wu LS, Chang HY, Shen CK. 2008. TDP-43, the signature protein of FTL-D-U, is a neuronal activity-responsive factor. *J Neurochem* 105:797–806.
- Warmus BA, Sekar DR, McCutchen E, Schellenberg GD, Roberts RC, McMahan LL, Roberson ED. 2014. Tau-mediated NMDA receptor impairment underlies dysfunction of a selectively vulnerable network in a mouse model of frontotemporal dementia. *J Neurosci* 34:16482–16495.

- Wegiel J, Wisniewski HM, Dziewiatkowski J, Tarnawski M, Dziewiatkowska A, Morys J, et al. 1996. Subpopulation of dogs with severe brain parenchymal beta amyloidosis distinguished with cluster analysis. *Brain Res* 728:20–26.
- Xiao X, Mruk DD, Tang EI, Massarwa R, Mok KW, Li N, Wong CK, Lee WM, Snapper SB, Shilo BZ, Schejter ED, Cheng CY. 2014. N-wasp is required for structural integrity of the blood-testis barrier. *PLoS Genet* 10:e1004447.
- Yoshino T, Uchida K, Tateyama S, Yamaguchi I, Nakayama H, Goto N. 1996. A retrospective study of canine senile plaques and cerebral amyloid angiopathy. *Vet Pathol* 33:230–234.
- Yu CH, Song GS, Yhee JY, Kim JH, Im KS, Nho WG, Lee JH, Sur JH. 2011. Histopathological and immunohistochemical comparison of the brain of human patients with Alzheimer's disease and the brain of aged dogs with cognitive dysfunction. *J Comp Pathol* 145:45–58.